

AD-A042 090

RIA-77-U1030

Cy No. 1

AD

A042090

USADACS Technical Library



5 0712 01001401 6

TECHNICAL
LIBRARY

OPTIMAL CONTROL OF ACTIVE RECOIL MECHANISMS

BY

S. M. WU

A. N. MADIWALE

February 1977

TECHNICAL REPORT



Prepared By

University of Wisconsin-Madison
Madison, Wisconsin 53706

DISTRIBUTION STATEMENT

Approved for public release, distribution unlimited.

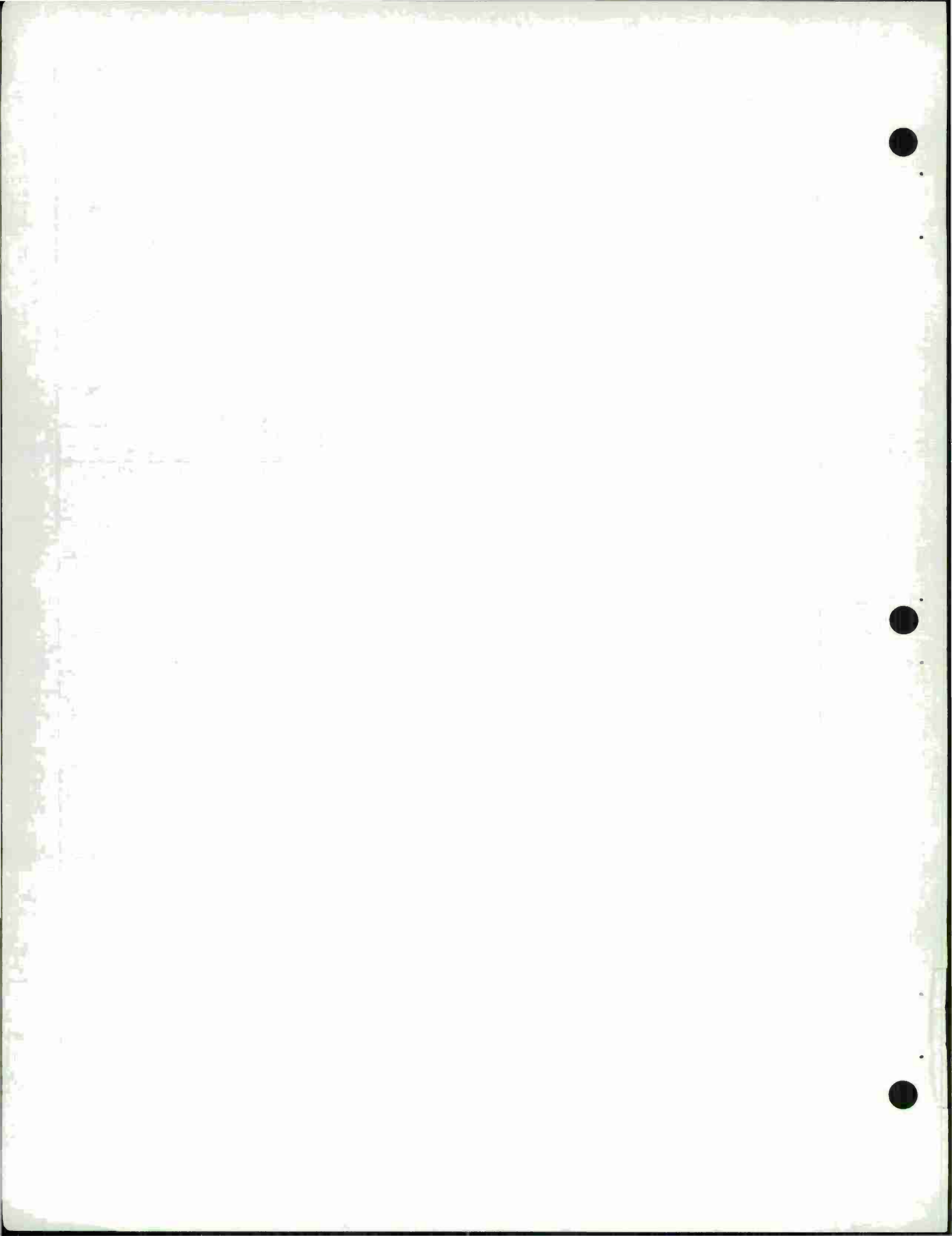
Prepared For
ENGINEERING DIRECTORATE

&

GENERAL THOMAS J. RODMAN LABORATORY

ROCK ISLAND ARSENAL
ROCK ISLAND, ILLINOIS 61201

| REPORT DOCUMENTATION PAGE | | READ INSTRUCTIONS BEFORE COMPLETING FORM |
|---|----------------------------|--|
| 1. REPORT NUMBER R-TR-77-024 | 2. GOVT ACCESSION NO. | 3. RECIPIENT'S CATALOG NUMBER |
| 4. TITLE (and Subtitle) Optimal Control of Active Recoil Mechanisms | | 5. TYPE OF REPORT & PERIOD COVERED Final June 1976 - December 1976 |
| | | 6. PERFORMING ORG. REPORT NUMBER |
| 7. AUTHOR(s) S.M. Wu A.N. Madiwale | | 8. CONTRACT OR GRANT NUMBER(s) DAAA09-76-M-2017 |
| 9. PERFORMING ORGANIZATION NAME AND ADDRESS University of Wisconsin-Madison Mechanical Engineering Department Madison, Wisconsin | | 10. PROGRAM ELEMENT, PROJECT, TASK AREA & WORK UNIT NUMBERS 1W161102AH55 |
| 11. CONTROLLING OFFICE NAME AND ADDRESS Engineering Directorate/Ware Simulation Division Rock Island Arsenal Rock Island, IL 61201 | | 12. REPORT DATE February 1977 |
| | | 13. NUMBER OF PAGES 80 |
| 14. MONITORING AGENCY NAME & ADDRESS (if different from Controlling Office) | | 15. SECURITY CLASS. (of this report) UNCLASSIFIED |
| | | 15a. DECLASSIFICATION/DOWNGRADING SCHEDULE |
| 16. DISTRIBUTION STATEMENT (of this Report) Approved for public release, distribution unlimited. | | |
| 17. DISTRIBUTION STATEMENT (of the abstract entered in Block 20, if different from Report) | | |
| 18. SUPPLEMENTARY NOTES | | |
| 19. KEY WORDS (Continue on reverse side if necessary and identify by block number) | | |
| 1. Recoil Mechanism | 5. Objective Function | |
| 2. Feedback | 6. Breech Force | |
| 3. Optimal Control | 7. Rod Pull | |
| 4. Servovalve | 8. Non-linear Optimization | |
| 20. ABSTRACT (Continue on reverse side if necessary and identify by block number) | | |
| <p>A servo-valve feedback system with variable control law is proposed for modification of a conventional hydropneumatic recoil mechanism to minimize peak recoil force for any round fired. Phase-plane-delta method of digital simulation is used to simulate the recoil mechanism model. An objective function with direct physical interpretations is developed and non-linear optimization techniques are used to design feedback gains for each firing round. The method is applied to M37 recoil mechanism and significant improvement in recoil force trajectories is obtained.</p> | | |



FOREWORD

This report was prepared by Prof. S. M. Wu and Mr. A. N. Madiwale of the University of Wisconsin-Madison in compliance with Contract No. DAAA09-76-M-2017. This work was performed for the Ware Simulation Division, Engineering Directorate, and the Research Directorate, GEN Thomas J. Rodman Laboratory, Rock Island, Illinois, with Mr. R. E. Kasten as Project Engineer

ACKNOWLEDGEMENT

This work was supported by the Ware Simulation Division, Engineering Directorate, Rock Island Arsenal, Rock Island, Illinois under Contract No. DAAA09-76-M-2017.

The authors developed their basic understanding of modeling recoil mechanisms through reports by Nerdahl and Frantz (8, 9, 10) and personal communications with the Ware Simulation Division. The suggestions by and discussions with Mr. Robert J. Radkiewicz and Mr. Robert E. Kasten of the Ware Simulation Division were very helpful and are deeply appreciated.

TABLE OF CONTENTS

| | <u>Page</u> |
|--|-------------|
| SUMMARY | xii |
| INTRODUCTION | 1 |
| I. MATHEMATICAL MODEL FOR HYDROPNEUMATIC RECOIL MECHANISM | 3 |
| II. DIGITAL SIMULATION OF THE MODEL | 10 |
| III. FORMULATION OF ADAPTIVE CONTROL AND OPTIMIZATION PROBLEM | 18 |
| 3.1 Linear State Feedback | 18 |
| 3.2 Development of Objective Function | 21 |
| 3.3 Results for M-102 | 27 |
| 3.4 Tachometer Feedback | 40 |
| CONCLUSIONS | 46 |
| Appendix I - Phase-Plane-Delta Digital Simulation Method | 48 |
| Appendix II - Nonlinear Optimization Algorithms | 54 |
| Appendix III - Design Data for M-37 Recoil Mechanism | 61 |

LIST OF FIGURES

| | | <u>Page</u> |
|----|--|-------------|
| 1 | Block Diagram of Conventional Recoil Mechanism | 4 |
| 2 | Phase Plane for Zone 7 | .12 |
| 3 | Displacement for Zone 7 | .13 |
| 4 | Velocity for Zone 7 | .14 |
| 5 | Rod Pull for Zone 7 | .15 |
| 6 | Cavitation Pressure for Zone 7 | .16 |
| 7 | Gas Pressure for Zone 7 | .17 |
| 8 | Block Diagram of Modified Recoil Mechanism | 19 |
| 9 | Rod Pull for Zone 7 With No Feedback . . . | .23 |
| 10 | Rod Pull for Zone 7 With Linear State Feedback 1 | .24 |
| 11 | Rod pull for Zone 8 With No Feedback . . . | .29 |
| 12 | Cavitation Pressure for Zone 8 With No Feedback | .30 |
| 13 | Rod Pull for Zone 8 With State Feedback . . | .31 |
| 14 | Cavitation Pressure for Zone 8 with Optimal Feedback | .32 |
| 15 | Rod Pull for Zone 7 With No Feedback . . . | .34 |
| 16 | Rod Pull for Zone 7 With Optimal Feedback . | .35 |
| 17 | Rod Pull for Zone 6 With No Feedback . . . | .36 |
| 18 | Rod Pull for Zone 6 With Optimal Feedback . | .37 |
| 19 | Rod Pull for Zone 5 With No Feedback . . . | .38 |
| 20 | Rod Pull for Zone 5 With Optimal Feedback . | .39 |

| | <u>Page</u> |
|----|--|
| 21 | Rod Pull for Zone 7 With Velocity Feedback 41 |
| 22 | Rod Pull for Zone 6 With Velocity Feedback 42 |
| 23 | Rod Pull for Zone 5 With Velocity Feedback 43 |
| 24 | Rod Pull for Zone 1 With Velocity Feedback 44 |
| 25 | Rod Pull for Zone 1 With No Feedback . . 45 |
| 26 | Phase Plane Method 49 |
| 27 | Phase Plane Delta Method 49 |
| 28 | Gradient Methods 56 |

LIST OF TABLES

| | <u>Page</u> |
|--|-------------|
| 1 Performance Parameters for Optimal Feedback Control | 28 |
| 2 Area of Variable Orifice of M37 Recoil Mechanism | 62 |
| 3 Breech Force for Zone 1 | 63 |
| 4 Breech Force for Zone 5 | 64 |
| 5 Breech Force for Zone 6 | 65 |
| 6 Breech Force for Zone 7 | 66 |
| 7 Breech Force for Zone 8 | 67 |

NOTATION

- A_R - Recoil rod area. in^2
- A_C - Control rod area. in^2
- A_D - Floating piston area. in^2
- A_N - Total area of floating piston = $A_C + A_D$. in^2
- A_1 - Area of orifice between recoil and recuperating chamber. in^2
- A_2 - Area of orifice between recuperating and control chamber. in^2
- $A_3(x)$ - Variable area of the groove in the floating piston at position x . in^2
- $B(t)$ - Breech force at time t . lbf
- C_1 - Discharge coefficient for orifice A_1 .
- C_2 - Discharge coefficient for orifice A_2 .
- C_3 - Discharge coefficient for orifice A_3 .
- C_q - Equivalent friction coefficient for frictional loss at orifices
- F_R - Dry friction at recoil piston.
- F_P - Dry friction at floating piston.
- F_q - Equivalent dry friction.
- g_1 - Position feedback gain.
- g_2 - Velocity feedback gain.
- g_3, g_4 - other feedback gains for nonlinear feedback.
- J - objective function

J_1
 J_2 }
 J_3 } - Components of objective function
 J_4 }
 J_5

m_p - Mass of the floating piston lbf sec²/in

m_R - Mass of the recoiling parts lbf sec²/in

m_q - Equivalent mass lbf sec²/in

P_0 - Initial gas pressure lbf/in²

P_G - Gas pressure at time t lbf/in²

R - Gas constant

$RDPL(t)$ - Rod pull at time t lbf

$RDPLD(t)$ - Desired Rod pull at time t lbf

T - Recoil time sec

$U(t)$ - Open area of servo valve in²

x - Position of recoiling parts with respect to
 recoil rod in

\dot{x} - Velocity of recoiling parts with respect to
 recoil rod in/sec

\ddot{x} - Acceleration of recoiling parts

y - Position of floating piston with respect to
 recoiling parts

w - Total weight of the recoiling parts.

w_q - Equivalent weight of recoiling parts.

w_1 }
 w_2 } - Weighting factors for components in the
 w_3 } objective function.
 w_4 }

α - The angle of elevation of the gun barrel radians

ρ - Mass density of the hydraulic fluid.

SUMMARY

Mathematical model for a conventional hydro-pneumatic recoil mechanism is developed from physical laws. This mathematical model is simulated on a digital computer by Phase-Plane-Delta method. The time histories of all pertinent parameters such as position of recoiling parts, hydraulic pressures in different chambers, rod pull are available and can be plotted.

A linear state feedback control system is proposed to adapt this conventional recoil mechanism to perform satisfactorily for all firing zones. The control and optimization problem is formulated. An objective function with direct relations to the performance and constraints of the problem is formulated. Davidon-Fletcher-Powell variable metric method of nonlinear optimization is used to design the feedback gains of the state feedback control law.

The above optimization procedure is applied to M-37 recoil mechanism for zone 5 through 8. This recoil mechanism originally was designed for zone 7. One set of feedback gains is designed for each zone and switching of control laws is suggested. A significant improvement in the recoil force time trajectory shape and reduction in peak force of 2.5 to 25 percent is obtained.

INTRODUCTION

Recoil mechanisms dissipate energy of the reaction of gunfire at a controlled rate so as to minimize the recoil force transferred to the carriage of a weapon system without exceeding available recoil length. Nerdahl and Frantz [9] have developed three degrees of freedom nonlinear models of hydropneumatic recoil mechanisms and a procedure to design a variable area orifice to control the energy dissipation. The procedure defines a control function or desired control recoil force-time trajectory for a design firing charge and with the help of digital simulation of the model, computes the orifice area at different positions of the recoil mechanism. This design performs satisfactorily for the designated firing charge, but far from optimum for other firing charges. Thus, a control system which can adapt to different firing zones is desirable.

A linear state feedback control system with variable gains is proposed in the report. A separate control law is designed for each firing charge and the control law corresponding to the charge being fired is selected from this predesigned set. This control scheme can be implemented by adding a servo valve operating in

tandem with the variable area orifice. The feedback gains for the servo valve can be selected from a predesigned set by identifying the charge being fired by sensing signals such as acceleration with the help of a microprocessor or special purpose digital electronics.

The design of the optimal control law is complicated by the highly nonlinear nature of the model induced by turbulent flow through orifices, dry friction at piston-cylinder surfaces and adiabatic gas compression. The nonlinear second order model is simulated on a digital computer using Phase-plane-delta method. A multifactor objective function with direct physical interpretation is developed as a function of the variables computed in the simulation. Davidon-Fletcher-Powell variable metric quasi-Newton nonlinear optimization algorithm is used to minimize the objective function. The procedure is applied to a M-37 105 mm recoil mechanism. Also, velocity feedback for lower zones 1, 5, and 6 is evaluated.

I

MATHEMATICAL MODEL FOR HYDROPNEUMATIC RECOIL MECHANISM

A schematic diagram for a conventional hydropneumatic recoil mechanism is shown in Fig. 1. A mathematical model based on the physical laws is developed with the following assumptions.

- 1) Flow through orifices is a potential flow.
- 2) Temperature variations do not affect the discharge coefficients for the orifice.
- 3) The recoil mechanism is secured to the carriage through a rigid link called the rod and the carriage rests on a rigid support.
- 4) Only translation of the recoil parts in direction of firing is considered.
- 5) There is no cavitation in any chamber.

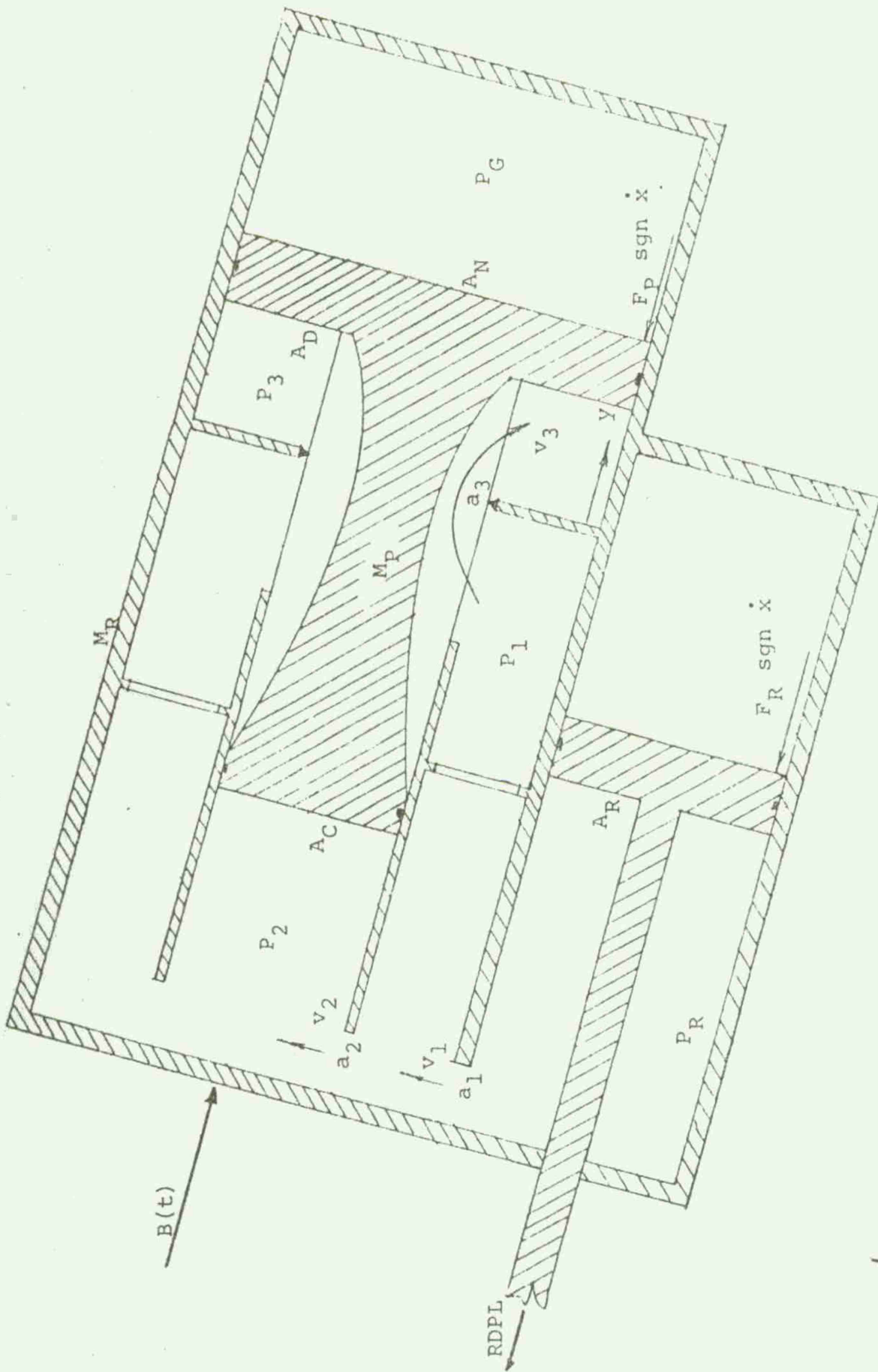


Figure 1. BLOCK DIAGRAM OF CONVENTIONAL RECOIL MECHANISM

PRESSURE RELATIONS

$$\begin{aligned}
 P_R - P_1 &= \left(\frac{\rho}{2}\right) \left(\frac{A_R}{A_1 C_1}\right)^2 \dot{x}^2 \operatorname{sgn} \dot{x} \\
 &= T_1 \dot{x}^2 \operatorname{sgn} \dot{x}
 \end{aligned} \tag{1}$$

$$\text{where } T_1 = \left(\frac{\rho}{2}\right) \left(\frac{A_R}{A_1 C_1}\right)^2$$

$$\begin{aligned}
 P_1 - P_2 &= \left(\frac{\rho}{2}\right) \left(\frac{A_C}{A_2 C_2}\right)^2 \dot{y}^2 \operatorname{sgn} \dot{y} \\
 &= \left(\frac{\rho}{2}\right) \left(\frac{A_C A_R}{A_2 C_2 A_N}\right)^2 \dot{x}^2 \operatorname{sgn} \dot{x} \\
 &= T_2 \dot{x}^2 \operatorname{sgn} \dot{x}
 \end{aligned} \tag{2}$$

$$\text{where } T_2 = \left(\frac{\rho}{2}\right) \left(\frac{A_C A_R}{A_2 C_2 A_N}\right)^2$$

$$\begin{aligned}
 P_1 - P_3 &= \left(\frac{\rho}{2}\right) \left(\frac{A_D}{C_3 A_3}\right)^2 \dot{y}^2 \operatorname{sgn} \dot{y} \\
 &= \left(\frac{\rho}{2}\right) \left(\frac{A_D A_R}{C_3 A_3 A_N}\right)^2 \dot{x}^2 \operatorname{sgn} \dot{x} \\
 &= T_3 \dot{x}^2 \operatorname{sgn} \dot{x}
 \end{aligned} \tag{3}$$

$$\text{where } T_3 = \left(\frac{\rho}{2}\right) \left(\frac{A_D A_R}{C_3 A_3 A_N}\right)^2$$

The gas pressure relation

$$P_G = P_0 \left(\frac{V_0}{V_0 - A_R \dot{x}} \right)^R \quad (4)$$

Thus the pressure equations are

$$P_R = P_1 + T_1 \dot{x}^2 \operatorname{sgn} \dot{x} \quad (1)$$

$$P_2 = P_1 - T_2 \dot{x}^2 \operatorname{sgn} \dot{x} \quad (2)$$

$$P_3 = P_1 - T_3 \dot{x}^2 \operatorname{sgn} \dot{x} \quad (3)$$

$$P_G = P_0 \left(\frac{V_0}{V_0 - A_R \dot{x}} \right)^R \quad (4)$$

Force balance for floating piston

$$\begin{aligned} m_p \left(1 + \frac{A_R}{A_N} \right) \ddot{x} &= m_p g \sin \alpha + A_D P_3 + A_C P_2 \\ &\quad - A_N P_G - F_p \operatorname{sgn} \dot{x} \end{aligned} \quad (5)$$

Substituting for P_R , P_2 , P_3 and P_G from equations 1, 2, 3, & 4 in 5 we have

$$\begin{aligned} m_p \left(1 + \frac{A_R}{A_N} \right) \ddot{x} &= m_p g \sin \alpha + A_D (P_1 - T_3 \dot{x}^2 \operatorname{sgn} \dot{x}) \\ &\quad + A_C (P_1 - T_2 \dot{x}^2 \operatorname{sgn} \dot{x}) - A_N P_0 \left(\frac{V_0}{V_0 - A_R \dot{x}} \right)^R - F_p \operatorname{sgn} \dot{x} \\ &= m_p g \sin \alpha - (A_D T_3 + A_C T_2) \dot{x}^2 \operatorname{sgn} \dot{x} \\ &\quad + (A_D + A_C) P_1 + m_p g \sin \alpha - A_N P_0 \left(\frac{V_0}{V_0 - A_R \dot{x}} \right)^R - F_p \operatorname{sgn} \dot{x} \end{aligned}$$

$$A_N P_1 = m_p \left(1 + \frac{A_R}{A_N}\right) \ddot{x} - m_p g \sin \alpha - (A_D T_3 + A_C T_2) \dot{x}^2 \operatorname{sgn} \dot{x} \\ + A_N P_0 \left(\frac{V_0}{V_0 - A_R x}\right)^R + F_p \operatorname{sgn} \dot{x} \quad (6)$$

Force balance for recoil mass

$$m_R \ddot{x} = B(t) + m_R g \sin \alpha - A_D P_3 - A_C P_2 + A_N P_G \\ + F_p \operatorname{sgn} \dot{x} - A_R P_R - F_R \operatorname{sgn} \dot{x} \quad (7)$$

Adding Equations (5) and (7) we have

$$\left[m_R + m_p \left(1 + \frac{A_R}{A_N}\right)\right] \ddot{x} = (m_p + m_R) g \sin \alpha + B(t) - \\ A_R P_R - F_R \operatorname{sgn} \dot{x} \quad (8)$$

Substituting for P_1 in Eq. (8) from Eq. (6) we have

$$\left[m_R + m_p \left(1 + \frac{A_R}{A_N}\right)\right] \ddot{x} = (m_p + m_R) g \sin \alpha + B(t) \\ - F_R \operatorname{sgn} \dot{x} - A_R T_1 \dot{x}^2 \operatorname{sgn} \dot{x} - \frac{A_R}{A_N} \left[m_p \left(1 + \frac{A_R}{A_N}\right) x - m_p g \sin \alpha\right] \\ + (A_C T_2 + A_D T_3) \dot{x}^2 \operatorname{sgn} \dot{x} + A_N P_0 \left(\frac{V_0}{V_0 - A_R x}\right)^R + F_p \operatorname{sgn} \dot{x} \\ = \left[m_R + m_p \left(1 + \frac{A_R}{A_N}\right)\right] g \sin \alpha + B(t) - (F_R + F_p \frac{A_R}{A_N}) \operatorname{sgn} \dot{x} \\ - \left[A_R T_1 + \frac{A_R}{A_N} (A_C T_2 + A_D T_3)\right] \dot{x}^2 \operatorname{sgn} \dot{x} - A_R P_0 \left(\frac{V_0}{V_0 - A_R x}\right)^R \\ - \frac{A_R}{A_N} m_p \left(1 + \frac{A_R}{A_N}\right) \ddot{x}$$

Finally

$$\begin{aligned}
 & [m_R + m_P (1 + \frac{A_R}{A_N})^2] \ddot{x} + [A_R T_1 + \frac{A_R}{A_N} (A_C T_2 + A_D T_3)] \dot{x}^2 \operatorname{sgn} \dot{x} \\
 & + A_R P_0 (\frac{V_0}{V_0 - A_R x})^R + (F_R + F_P \frac{A_R}{A_N}) \operatorname{sgn} \dot{x} \\
 & = [m_R + m_P (1 + \frac{A_R}{A_N})] g \sin \alpha + B(t)
 \end{aligned} \tag{9}$$

Let

m_q - equivalent mass

$$= m_R + m_P (1 + \frac{A_R}{A_N})^2$$

C_q - equivalent damping coefficient

$$= [A_R T_1 + \frac{A_R}{A_N} (A_C T_2 + A_D T_3)]$$

F_q - equivalent dry friction

$$= (F_R + F_P \frac{A_R}{A_N})$$

W_q - equivalent weight

$$= [m_R + m_P (1 + \frac{A_R}{A_N})] g \sin \alpha$$

Thus equation (9) can be rewritten as

$$\begin{aligned}
 & m_q \ddot{x} + C_q \dot{x}^2 \operatorname{sgn} \dot{x} + F_q \operatorname{sgn} \dot{x} + A_R P_0 (\frac{1}{1 - \frac{A_R}{V_0} x})^R \\
 & = W_q + B(t)
 \end{aligned} \tag{10}$$

Note - C_q is not a constant and is a function of the position of the floating piston due to the variable orifice area A_3 .

The rod pull is

$$RDPL = P_R A_R + F_R \operatorname{sgn} \dot{x} \quad (11)$$

From equations (8) and (11) we have

$$RDPL = -[m_R + m_P (1 + \frac{A_R}{A_N})] \ddot{x} + (m_P + m_R)g \sin \alpha + B(t) \quad (12)$$

Thus equation (10) is the final model of the form

$$m\ddot{x} + (a+f(x))\dot{x}^2 \operatorname{sgn} \dot{x} + k(1-a_0 x)^{-R} = W + B(t)$$

and equations 1, 2, 3, 4, and 12 are relations for all pertinent variables.

II

DIGITAL SIMULATION OF RECOIL MECHANISM MODEL

The nonlinear second order model developed in Section I Equation (10) can be simulated on a high speed digital computer by phase-plane-delta method. This method transforms a forced nonlinear model into a linear oscillator for a short interval of time and is explained in detail in Appendix I. The simulation results in time histories of all the pertinent variables such as position, velocity, rod pull, and all the pressures. This method is computationally very efficient.

The model in equation (10) can be reformulated in phase-plane-delta format as follows

$$m_q \ddot{x} + c_q \dot{x}^2 \operatorname{sgn} \dot{x} + A_R P_0 \left(1 - \frac{A_R}{V_0} x\right)^{-R} + F_q \operatorname{sgn} \dot{x} = W_q + B(t)$$

or

$$\ddot{x} + p^2 (x + \delta x) = 0 \quad (13)$$

where

$$\delta x = -x + \frac{1}{p^2 m_q} \left\{ C_q \dot{x}^2 \operatorname{sgn} \dot{x} + A_R P_0 \left(1 - \frac{A_R}{V_0} x\right)^{-R} + F_q \operatorname{sgn} \dot{x} - W_q - B(t) \right\} \quad (14)$$

From initial conditions $x_0 = 0$, $\dot{x}_0 = 0$, the simulation is started and run until the recoil mechanism starts counter-recoil.

A fortran program is written to simulate the recoil

mechanism based on equations (13) and (14).

An example simulation was run for M-37 recoil mechanism zone 7 firing charge. The phase plane, x , \dot{x} , P_3 , P_G , and rod pull are plotted in Figures 2, 3, 4, 5, 6, and 7.

The simulation results are in agreement with a digital simulation run by the Ware Simulation Division at Rock Island Arsenal using Continuous System Modeling Program (CSMP).

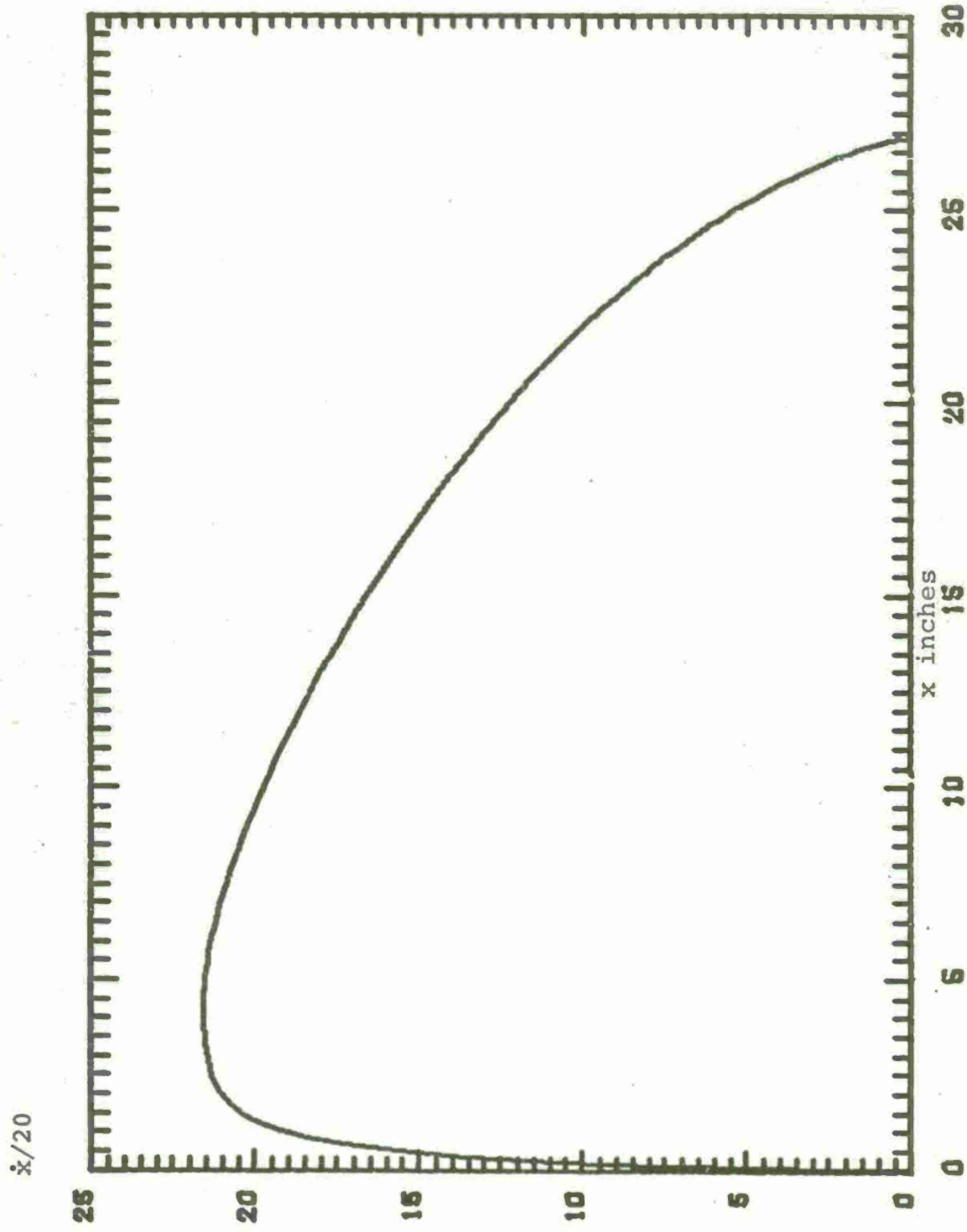


Figure 2 Phase plane for Zone 7

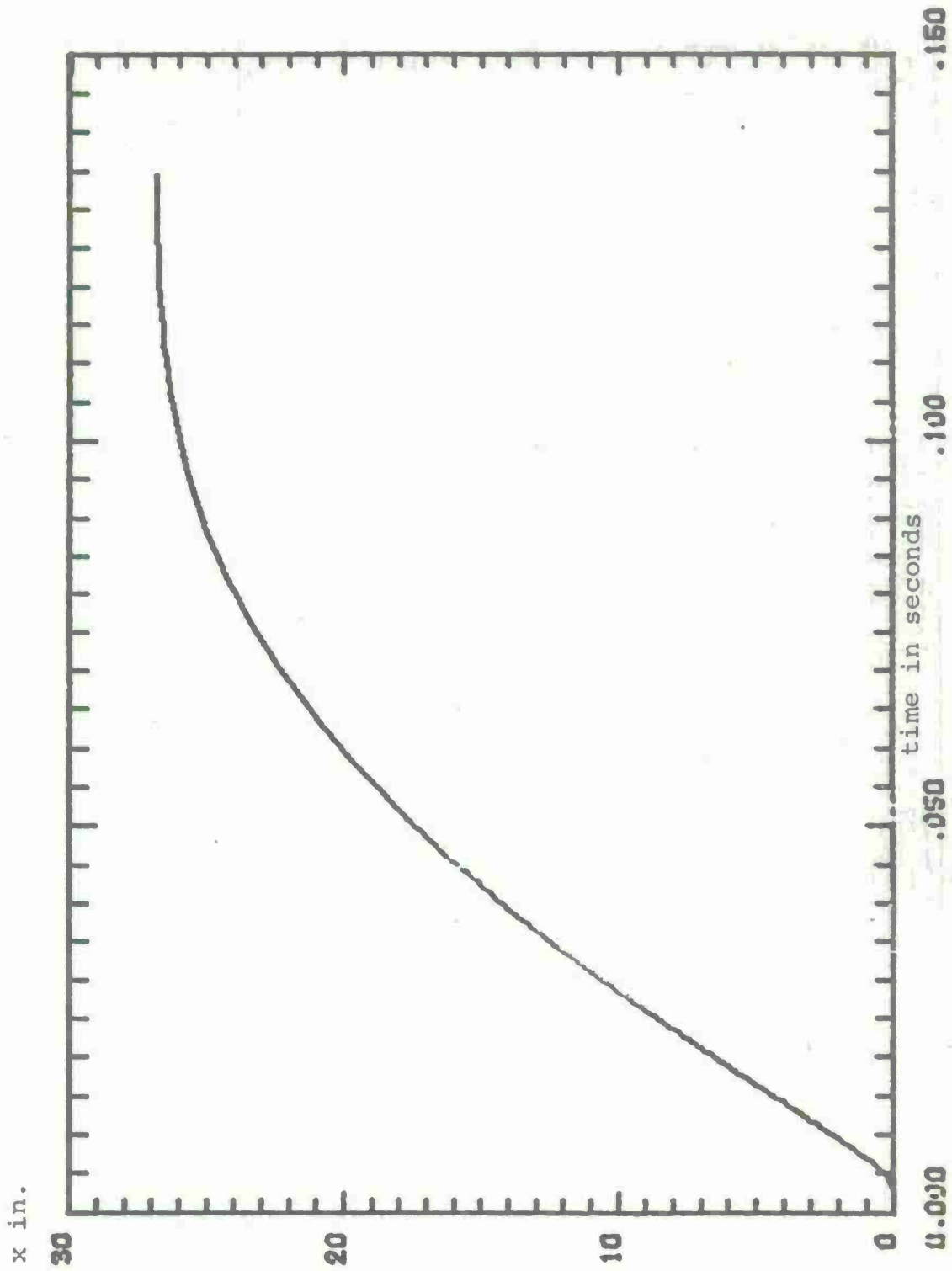


Figure 3 Displacement for Zone 7

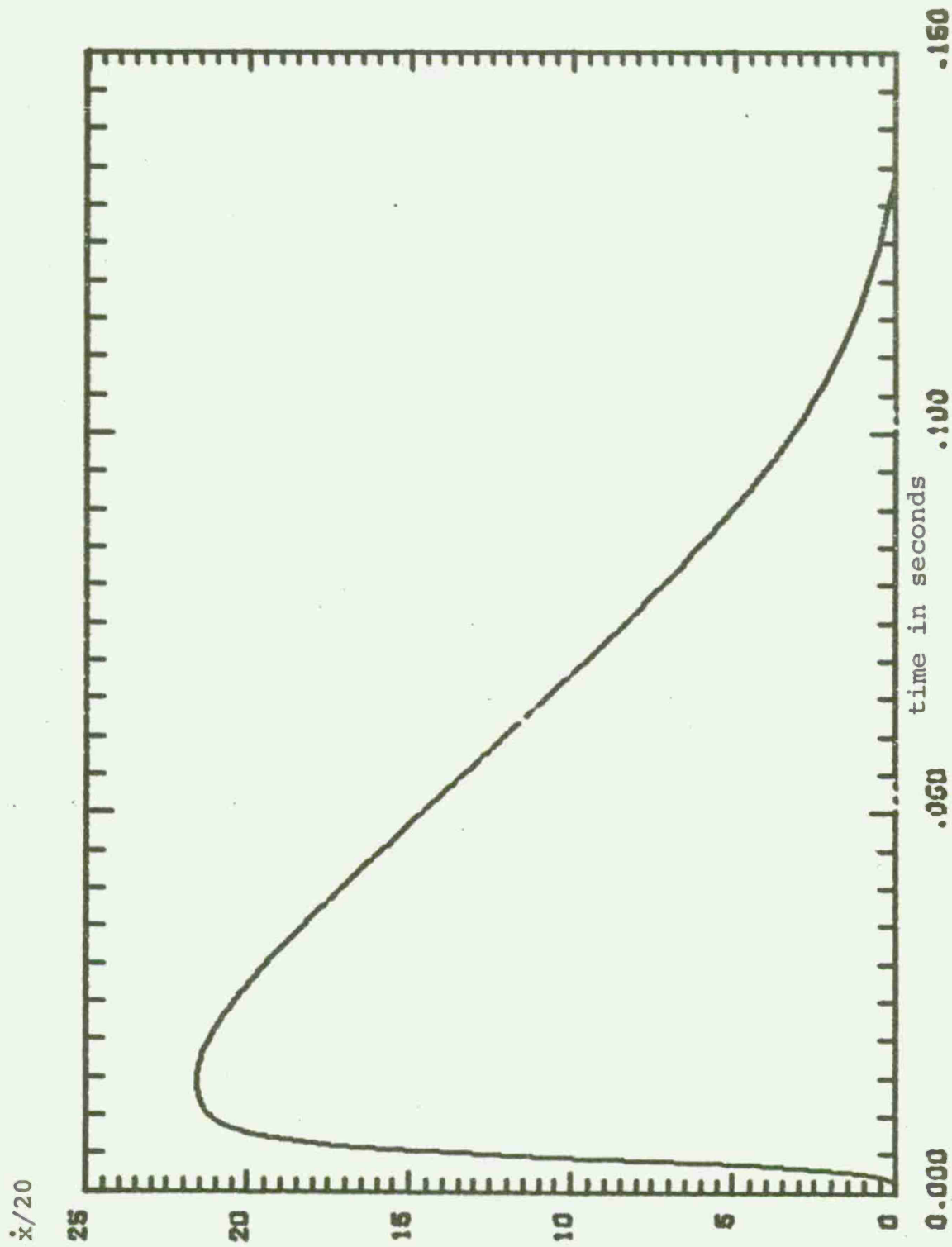


Figure 4 Velocity for Zone 7

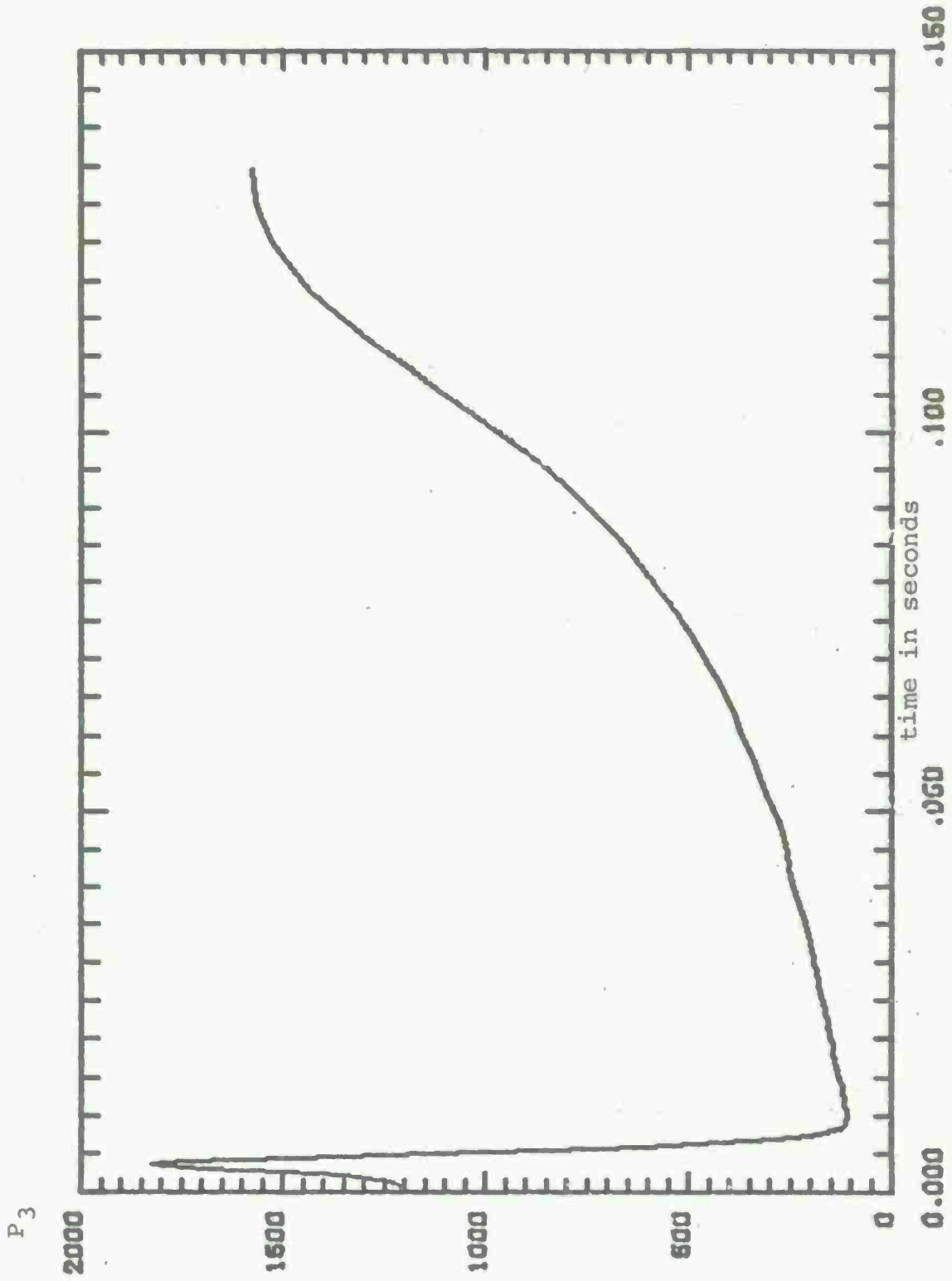


Figure 5 Cavitation Pressure for Zone 7

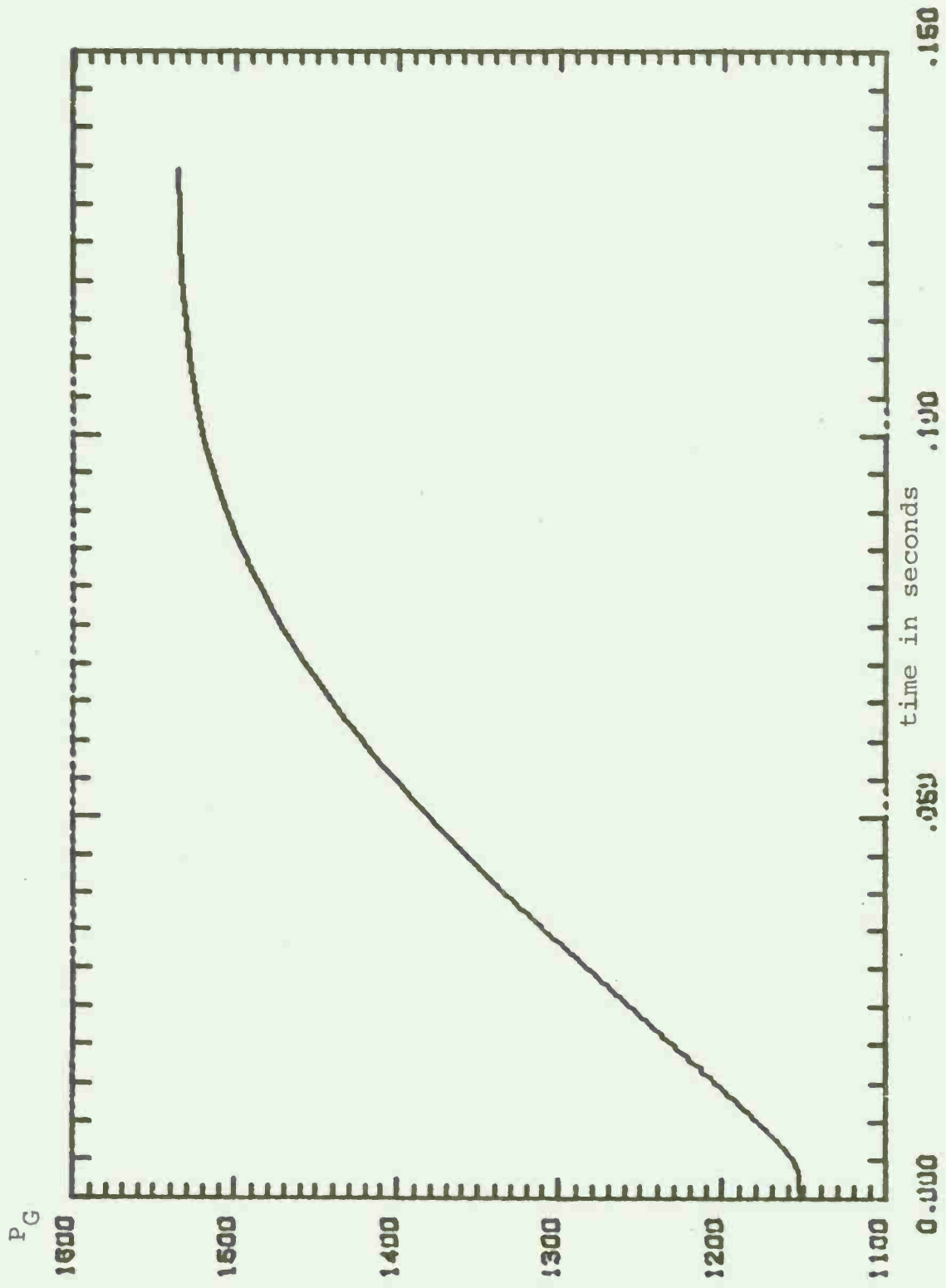


Figure 6 Gas Pressure for Zone 7

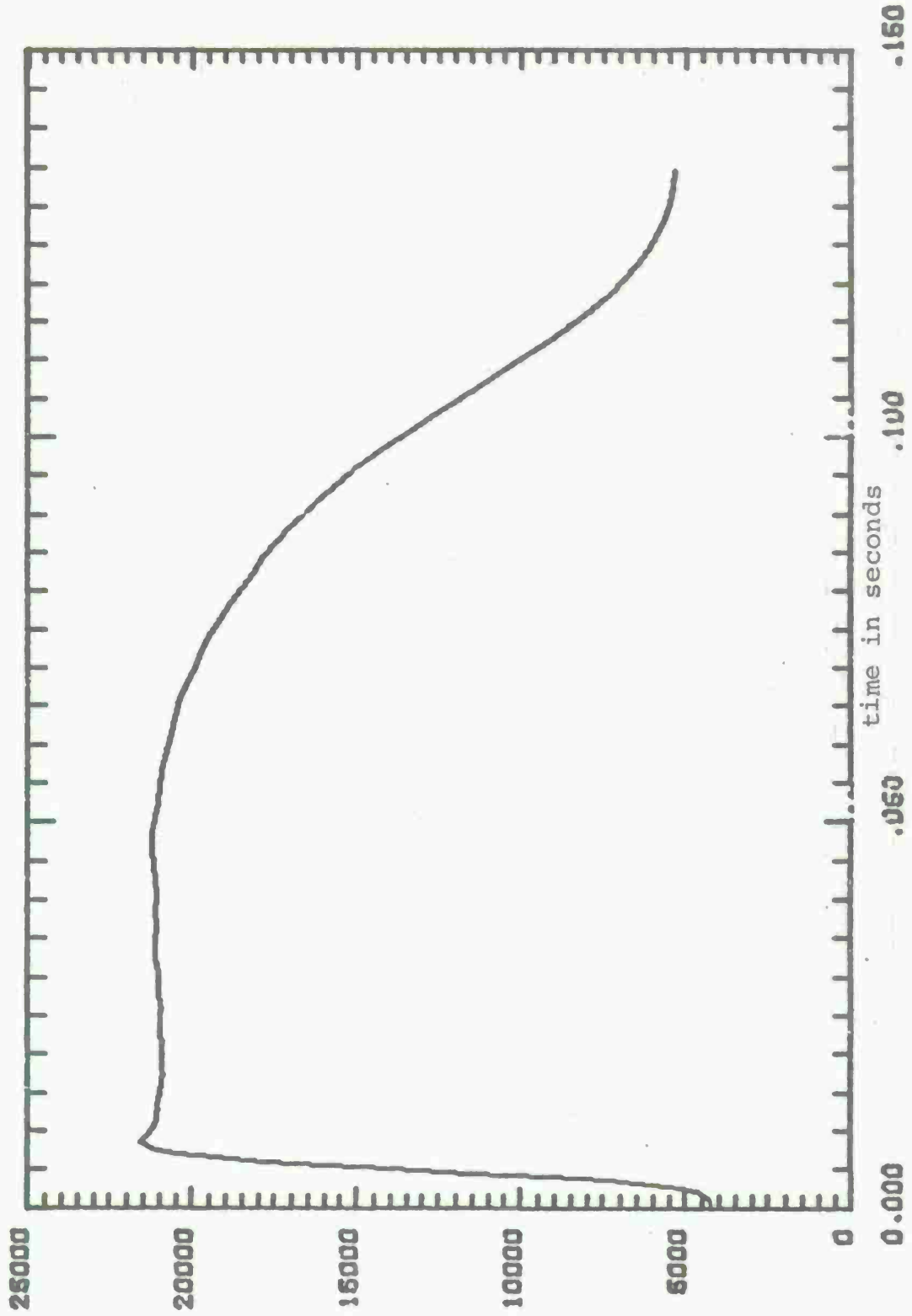


Figure 7 Rod Pull for Zone 7

III

FORMULATION OF ADAPTIVE CONTROL AND OPTIMIZATION PROBLEM

The control groove machined in the floating piston is designed for a designated zone and performs satisfactorily when used for the design zone. The purpose of this research is to adapt the recoil mechanism such that it adapts to the charges being fired so as to perform satisfactorily without violating the system constraints. A modified design of the recoil mechanism with a servo valve operating in tandem with the variable area groove is shown in Figure 8. The area of the servo valve that is open for the flow of hydraulic fluid is controlled by a feedback law. The feedback law can be changed by sensing the zone being fired. This adds the flexibility to change and adapt to the firing zone.

3.1 Linear State Feedback

A linear state feedback control is proposed to control the area of the servo valve and is of the form

$$u = g_1x + g_2\dot{x} \quad (15)$$

where g_1 and g_2 are feedback gains and u is the area of the servo valve. The corresponding modification in the mathematical model is in the equivalent damping coefficient C_q as follows

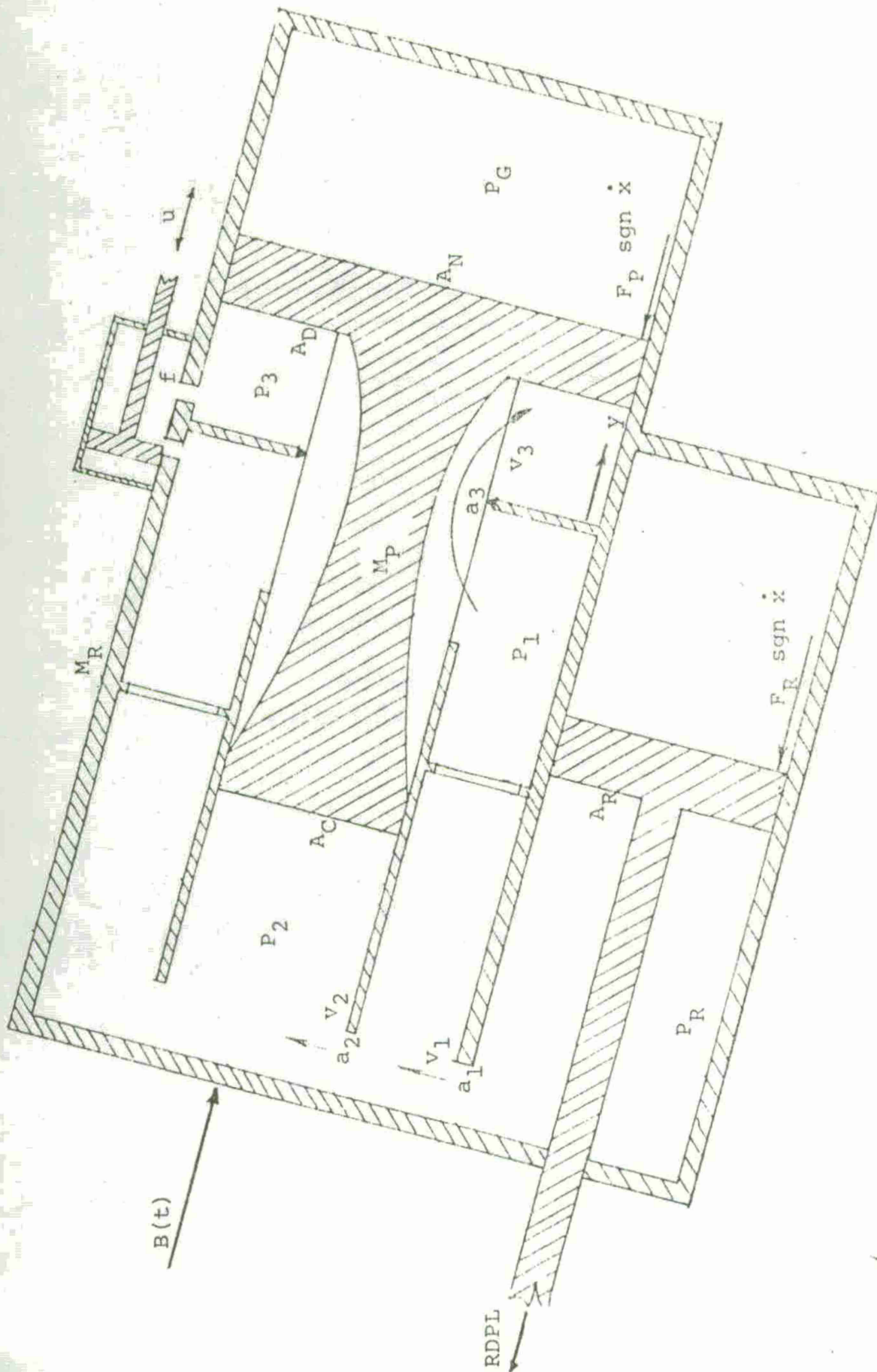


Figure 8. BLOCK DIAGRAM OF MODIFIED RECOIL MECHANISM

$$C_q = A_R T_1 + \frac{A_R}{A_N} (A_C T_2 + A_D T_3)$$

and

$$T_3 = \left(\frac{\rho}{2}\right) \left(\frac{A_0}{C_3} \frac{A_R}{A_N (A_3 + u)}\right)^2 \quad (16)$$

The modified form of the model is

$$\begin{aligned} m\ddot{x} + [a + f(x) + u(x, \dot{x})] \dot{x}^2 \operatorname{sgn} \dot{x} + k(1 - a_0 x)^{-R} + F \operatorname{sgn} \dot{x} \\ = W + B(t) \end{aligned}$$

The task of finding optimal values g_1 and g_2 of the feedback gains is formulated as follows.

Find optimal values of g_1 and g_2 such that an objective function $J(g_1, g_2)$ is minimized subject to the following constraints. The system follows the model

$$1) \quad m_q \ddot{x} + C_q \dot{x}^2 \operatorname{sgn} \dot{x} + F_q \operatorname{sgn} \dot{x} + A_R P_0 \left(1 - \frac{A_R}{V_0} x\right)^{-R} = W_q + B(t)$$

where

$$C_q = A_R T_1 + \frac{A_R}{A_N} (A_C T_2 + A_D T_3)$$

$$T_3 = \left(\frac{\rho}{2}\right) \left(\frac{A_0}{C_3} \frac{A_R}{A_N}\right)^2 \frac{1}{(A_3 + g_1 x + g_2 \dot{x})^2}$$

- 2) X_{\max} , the maximum recoil length
 $\leq X_m$, the available recoil length
- 3) There is no cavitation in chamber 3, i.e.,
 $P_3(t) \geq P_3 \min$

- 4) The maximum servovalve area $u = g_1 x + g_2 \dot{x}$

$$U_{\max} \leq U_m$$

3.2 Development of an Objective Function

The basic performance criterion is that the actual rod pull trajectory should follow as closely as possible the desired control trajectory for every zone. So let the control trajectory be RDPLD(t)

Then,

$$J(g_1, g_2) = \int_0^T [\text{RDPLD}(t) - \text{RDPL}(t)]^2 dt$$

will represent the integrated error or least square error criterion. To be able to use unconstrained optimization techniques, penalty functions can be added to take care of constraints and hence the penalty functions are

$$J_2 = \int_0^T w_2 (P_3(t) - P_{3 \min})^2 dt$$

$$J_3 = \int_0^T w_3 (U(t) - U_m)^2 dt$$

$$J_4 = \int_0^T w_4 (x - x_m)^2 dt$$

where $w_2 = 0 \quad P_3(t) > P_{3 \min}$

$$w_3 = 0 \quad U(t) < U_m$$

$$w_4 = 0 \quad x < x_m$$

So the composite objective function is

$$J(g_1, g_2) = \int_0^T \{ w_1 (\text{RDPLD}(t) - \text{RDPL}(t))^2 + w_2 (P_3(t) - P_{3 \text{ min}})^2 + w_3 (U(t) - U_m)^2 + w_4 (x - x_m)^2 \} dt$$

By choosing w_2, w_3, w_4 large positive numbers, the constraint violations can be avoided.

The VA10A optimization routine available on UNIVAC 1110 at UWMACC which uses Davidon - Fletcher - Powell (Appendix III) method was used to find optimal values of g_1, g_2 for zone 7 and results are shown in figure 9, 10. The control trajectory was chosen arbitrarily. Figure 9 is with no feedback and 10 is with optimal feedback gains of $g_1 = .2742E-3$ and $g_2 = .354E-7$. The actual trajectory follows the desired trajectory in Fig. 10 more closely than in Fig. 9.

The procedure was repeated for other zones with arbitrary control trajectory. The optimization procedure is very sensitive to the definition of the control trajectory and thus redefinition of the objective function without the control trajectory is necessary. The main objective can be reiterated as the minimization of rod pull and a flat trajectory to avoid sudden or sharp changes which induce fatigue failure. The first derivative represents the smoothness or flatness of the trajectory to some extent and hence, a penalty for large first derivatives can be added to the objective function.

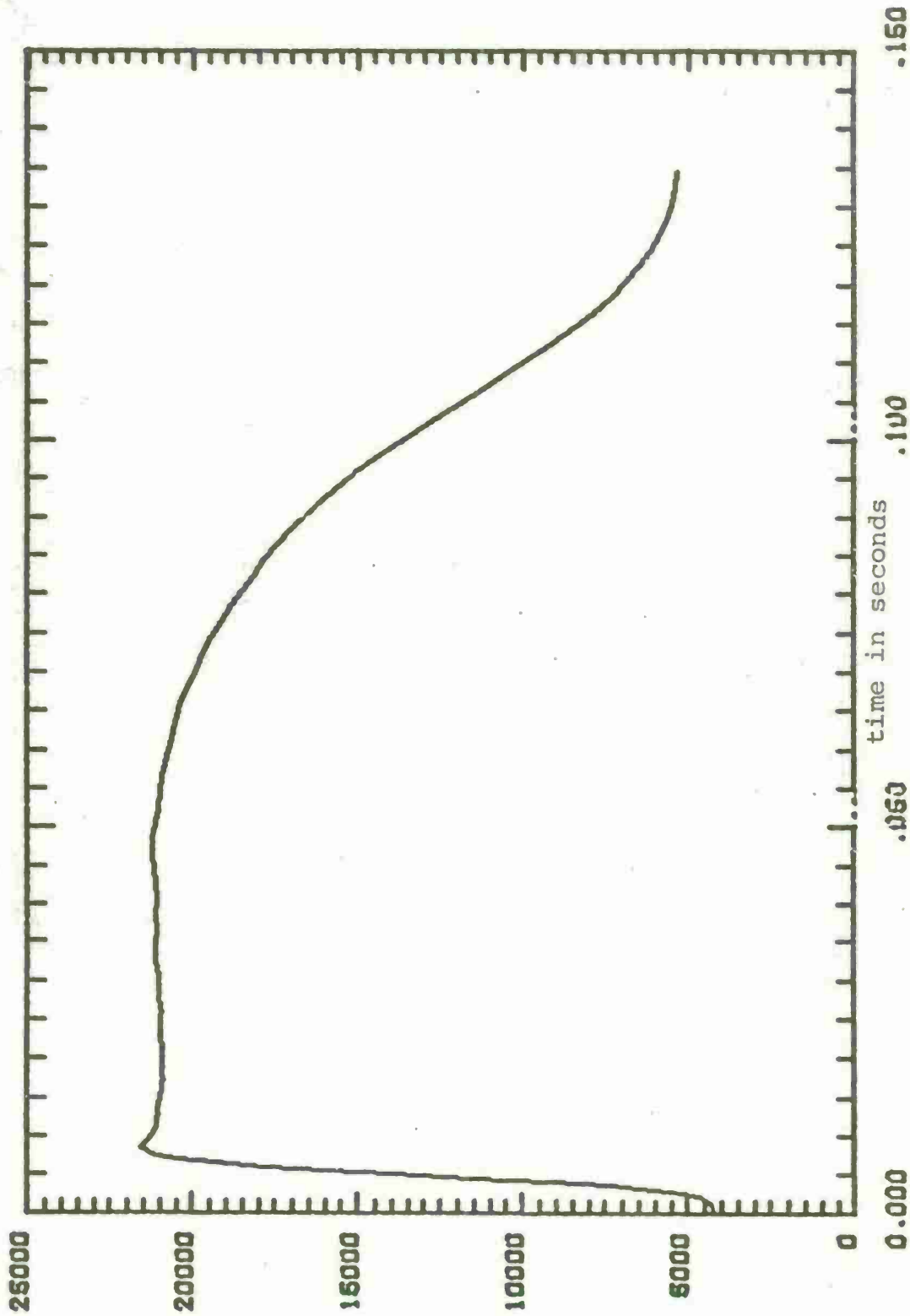


Figure 9 Rod Pull for Zone 7 with No Feedback

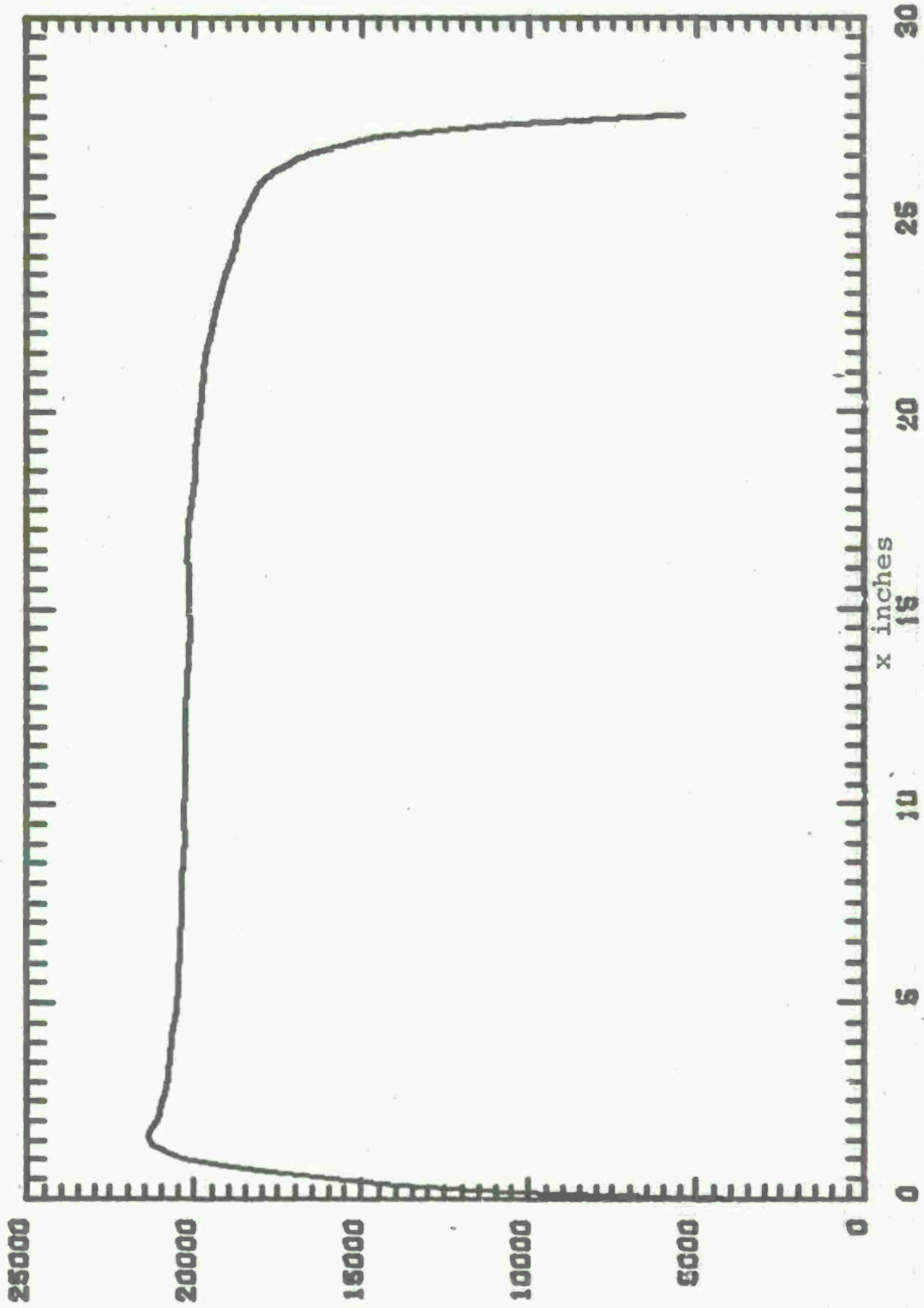


Figure 10 Rod Pull for Zone 7 With Linear Feedback i.

The new composite objective function can be written in five parts as

$$J_1 = \int_0^T (\text{RDPL}(t) - C)^2 dt$$

where C is a constant = 4200.

Penalty for non-smoothness

$$J_2 = \int_0^T \left\{ \frac{\partial}{\partial t} \text{RDPL}(t) \right\}^2 dt$$

Penalty for constraint violation for cavitation

$$J_3 = \int_0^T (P_3(t) - P_{3 \text{ min}})^2 dt$$

Penalty for maximum servo-valve area constraint

$$J_4 = \int_0^T (U(t) - U_m)^2 dt$$

Penalty for maximum recoil length constraint

$$J_5 = \int_0^T (X - X_m)^2 dt$$

The composite objective function being

$$J = w_1 J_1 + w_2 J_2 + w_3 J_3 + w_4 J_4 + w_5 J_5$$

$$\text{with } w_3 = 0 \text{ if } P_3(t) > P_{3 \text{ min}}$$

$$w_4 = 0 \text{ if } U(t) \leq U_m$$

$$w_5 = 0 \text{ if } X < X_m$$

The weighting factors w_1 and w_2 provide a trade off between the minimum error and flatness of the rod pull trajectory. Large w_1 with respect to w_2 will result in sharp trajectory with a peak in initial stage of recoil.

Large w_2 with respect to w_1 will result in a sharp peak at a later stage in recoil and also possibly will result in cavitation at variable area orifice 3. By choosing w_1 and w_2 in between these extremes, a satisfactory shape of the trajectory can be achieved.

The weighting factors w_3 , w_4 , and w_5 emphasize or de-emphasize the penalty functions for constraint violations. If any constraint is violated, the corresponding weighting factor can be increased so as to force the optimization algorithm to choose a feasible solution.

3.3 Results for M-37 Recoil Mechanism

The linear state feedback control system and optimization procedure discussed in Sections 3.1 and 3.2 was applied to M-37 recoil mechanism. M-37 was designed for a firing charge zone 7. The design data and breech forces for zones 1, 5, 6, 7, and 8 are tabulated in Appendix III and was provided by the Ware Simulation Division at Rock Island Arsenal. The breech forces used are from simulated breech forces. The breech force for zone 8 was arrived at by multiplying breech force for zone 7 by 1.2 due to unavailability of data.

The feedback gains for zones 5, 6, 7, and 8 and other parameters are presented in Table 1. The rod pull characteristics are plotted in Figures 11 through 20 with no feedback and with optimal feedback.

Figures 11 and 13 portray the time history of the rod pull for no feedback and optimum linear feedback control for zone 8. Zone 8 was arrived at by multiplying zone 7 breech force by 1.2. Though the trajectory for no feedback looks very satisfactory, the Figure 12 which plots the pressure $P_3(t)$ reveals that there is cavitation and hence the model is no longer valid. Figure 13 shows trajectory not very flat but there is no cavitation as shown in Fig. 14. This is achieved through optimization with penalty for cavitation. With Random

Table 1 Results of Optimum Feedback for Zones 5, 6, 7 and 8

| Zone | Gains | | Recoil Length (in) | Recoil Time (sec) | Rod Pull Maximum (lbs) | Servo Value Area Maximum (in ²) |
|------|----------|---------|--------------------|-------------------|--|---|
| | g_1 | g_2 | | | | |
| 8 | 0 | 0 | 27 | .126 | 25,200 Cavitation | 0 |
| 8 | .81E-4 | .884E-5 | 27.6 | .12 | 25,800 No Cavitation | .005 |
| 7 | 0 | 0 | 27 | .13 | Max ^m 21,500 Flat 21,000 | 0 |
| 7 | .1803E-3 | .532E-5 | 27.6 | .13 | Max ^m 21,000 Flat 20,500 | .0054 |
| 6 | 0 | 0 | 25.8 | .17 | 14,700 | 0 |
| 6 | .17E-3 | .376E-4 | 27.2673 | .158 | 12,900 | .0134 |
| 5 | 0 | 0 | 24 | .19 | 11,360 | 0 |
| 5 | .6591E-3 | .1E-3 | 28.1647 | .194 | Max ^m 8,800 Flat 8,500 | .032 |

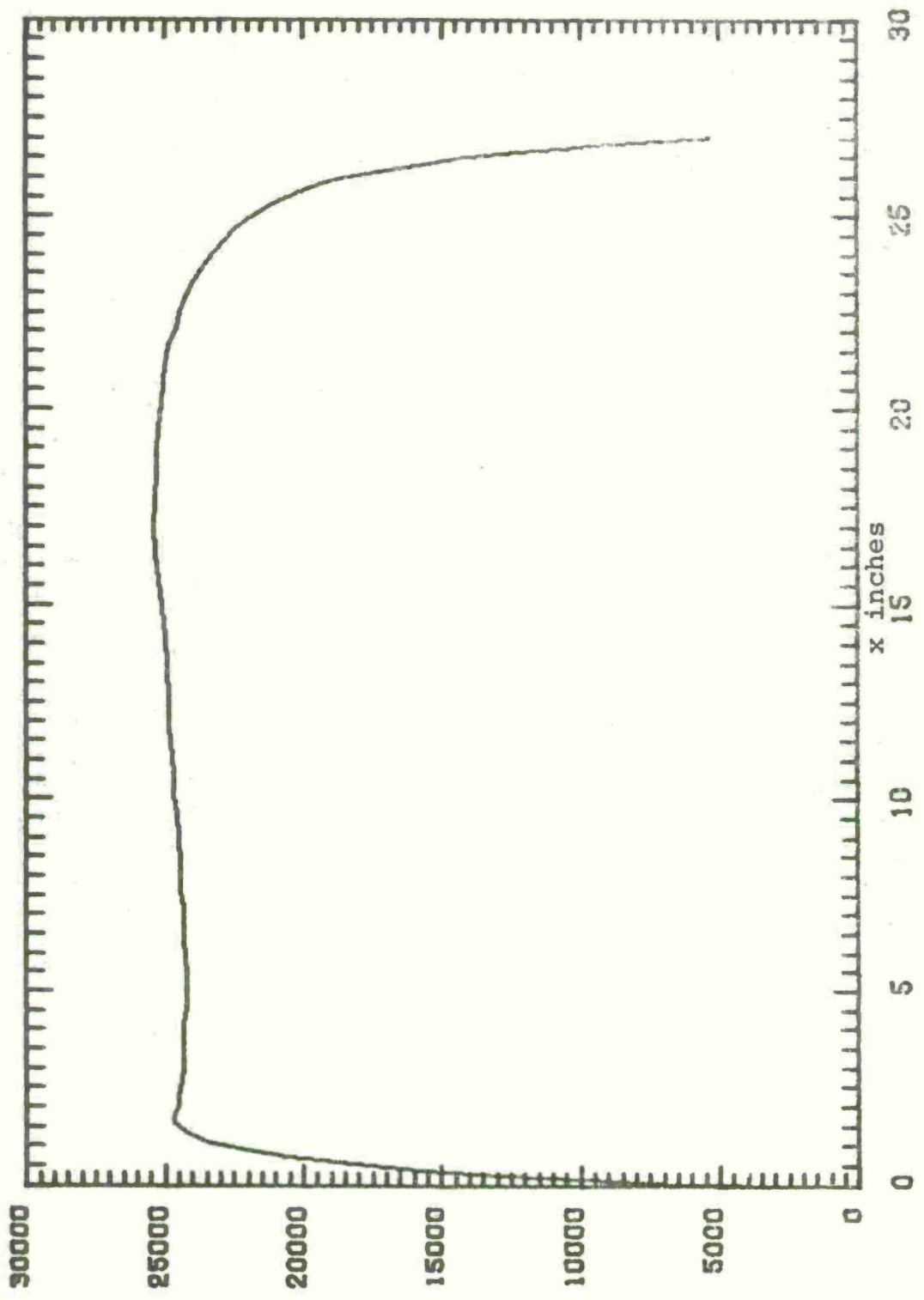


Figure 11 Rod Pull for Zone 8 with No Feedback

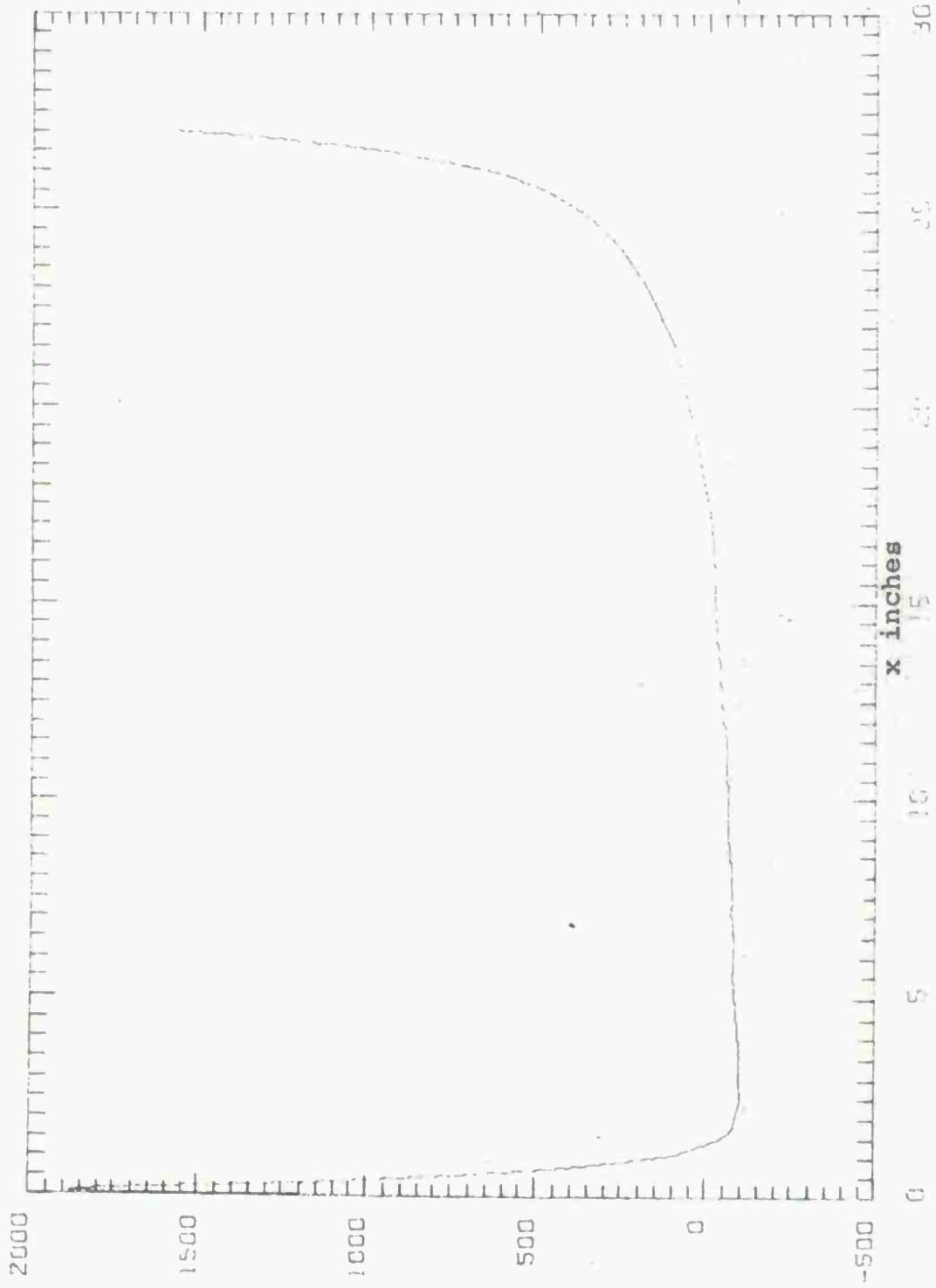


Figure 12 Cavitation Pressure for Zone 8 with No Feedback

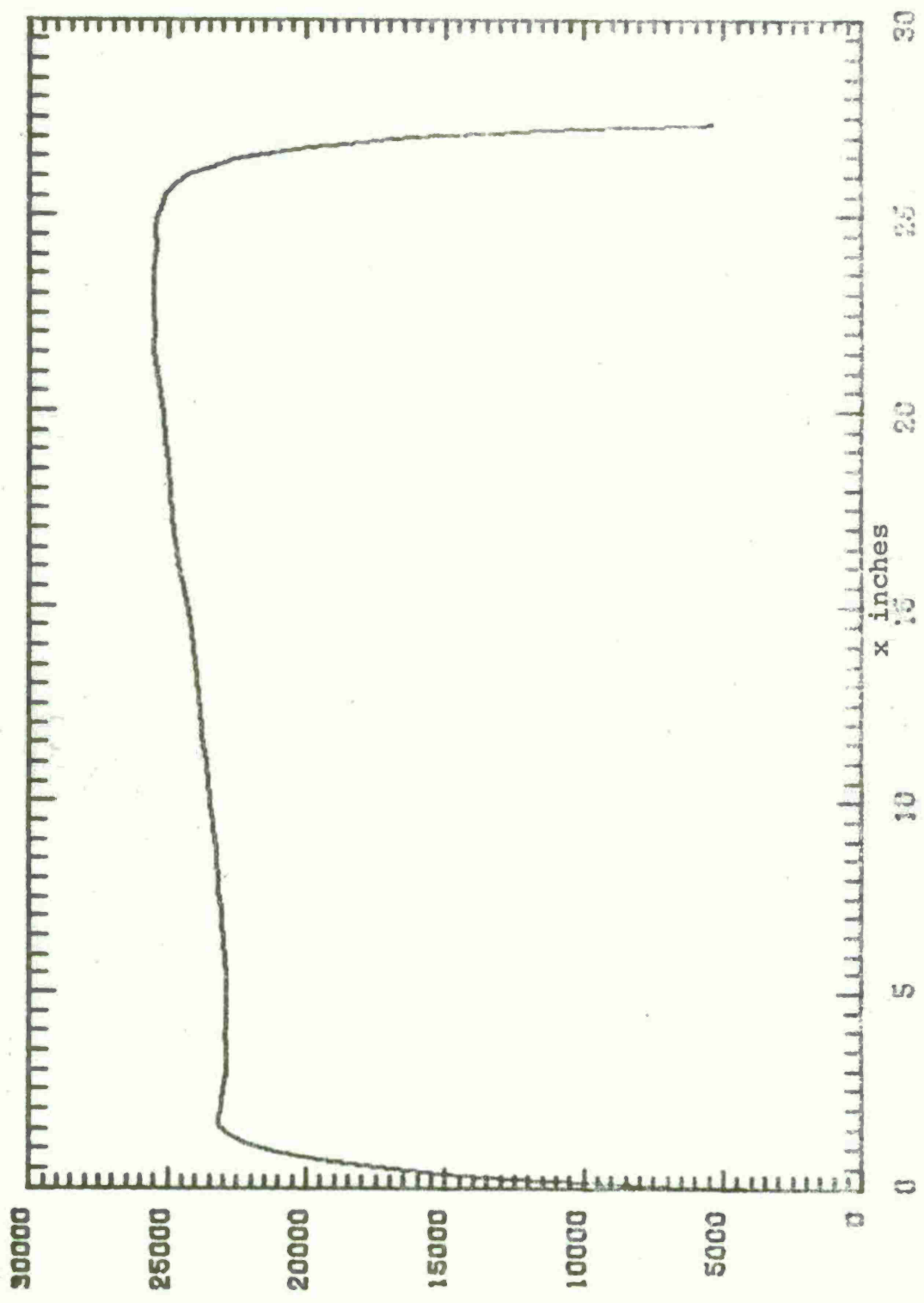


Figure 13 Rod Pull for Zone 8 with Feedback

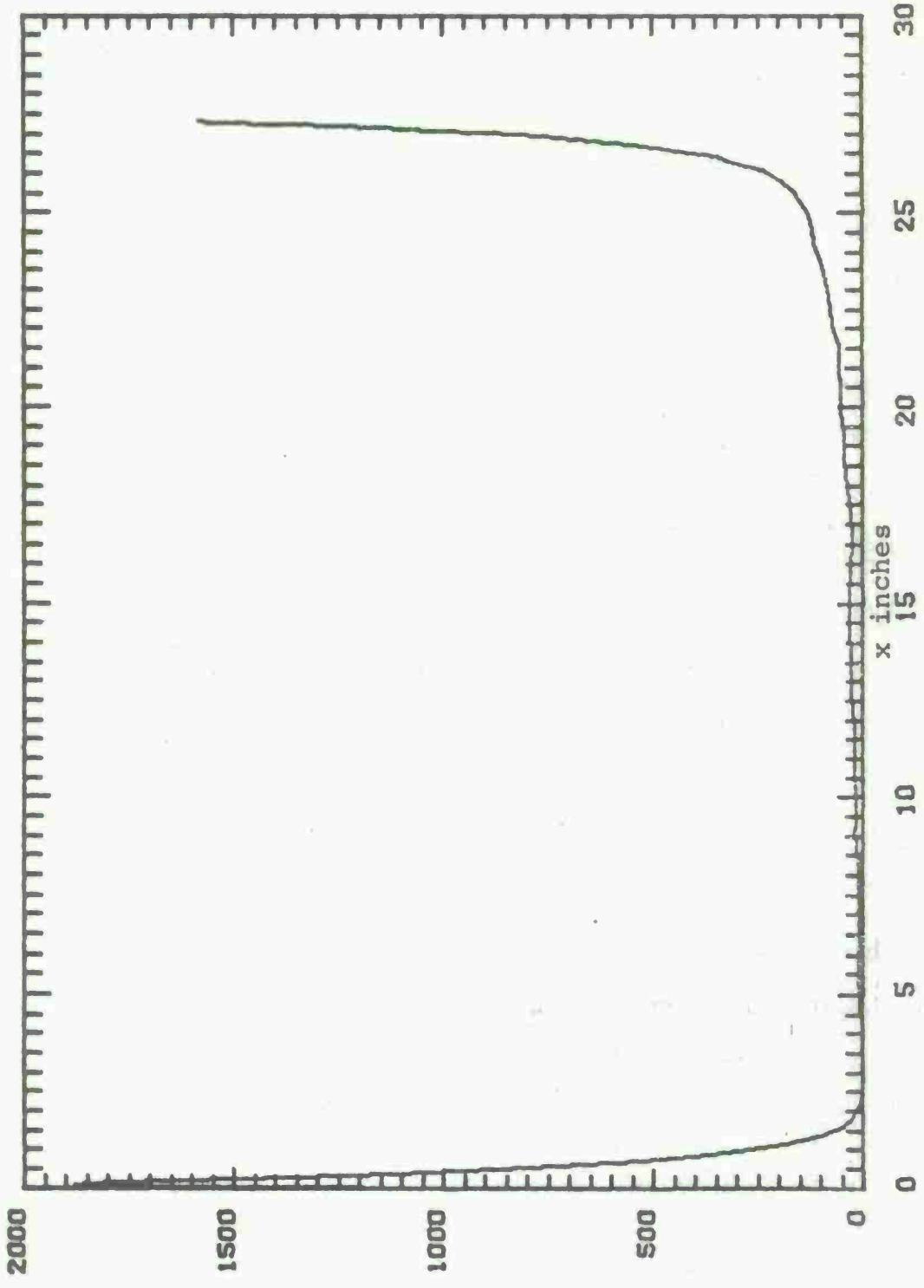


Figure 14 Cavitation Pressure for Zone 8 with Feedback

Search technique P_3 min was increased up to 20 psi. With reasonable P_3 min, cavitation can completely be eliminated.

Figures 15 and 16 are rod pull trajectories for zone 7 with no feedback and with optimal feedback. The improvement is not significant. The improvement was significant as shown in Figures 9 and 10 even for zone 7 with the first objective function. The relative improvement in peak force is about 2.5% and recoil length is longer by 0.6 inches. There is no change in the total recoil time of .13 seconds.

The rod pull trajectory for zone 6 with no feedback is a more triangular with maximum rod pull of 14,700 lbs. (Figure 17). The optimal feedback control law results in a very flat trajectory with maximum force of 12,900 which is a significant reduction of about 12% (Figure 18). The recoil length is increased from 25.8 inches to 27.27 inches but recoil time is reduced from .17 seconds to .158 seconds.

The rod pull trajectory for zone 5 with no feedback is a sharp triangular one with peak of 11,360 lbs. (Figure 19). The optimal feedback control law reduces this force to 8500 lbs with a flat and trapezoidal trajectory. The recoil length and time are both increased. The percentage reduction in recoil force is 25%.

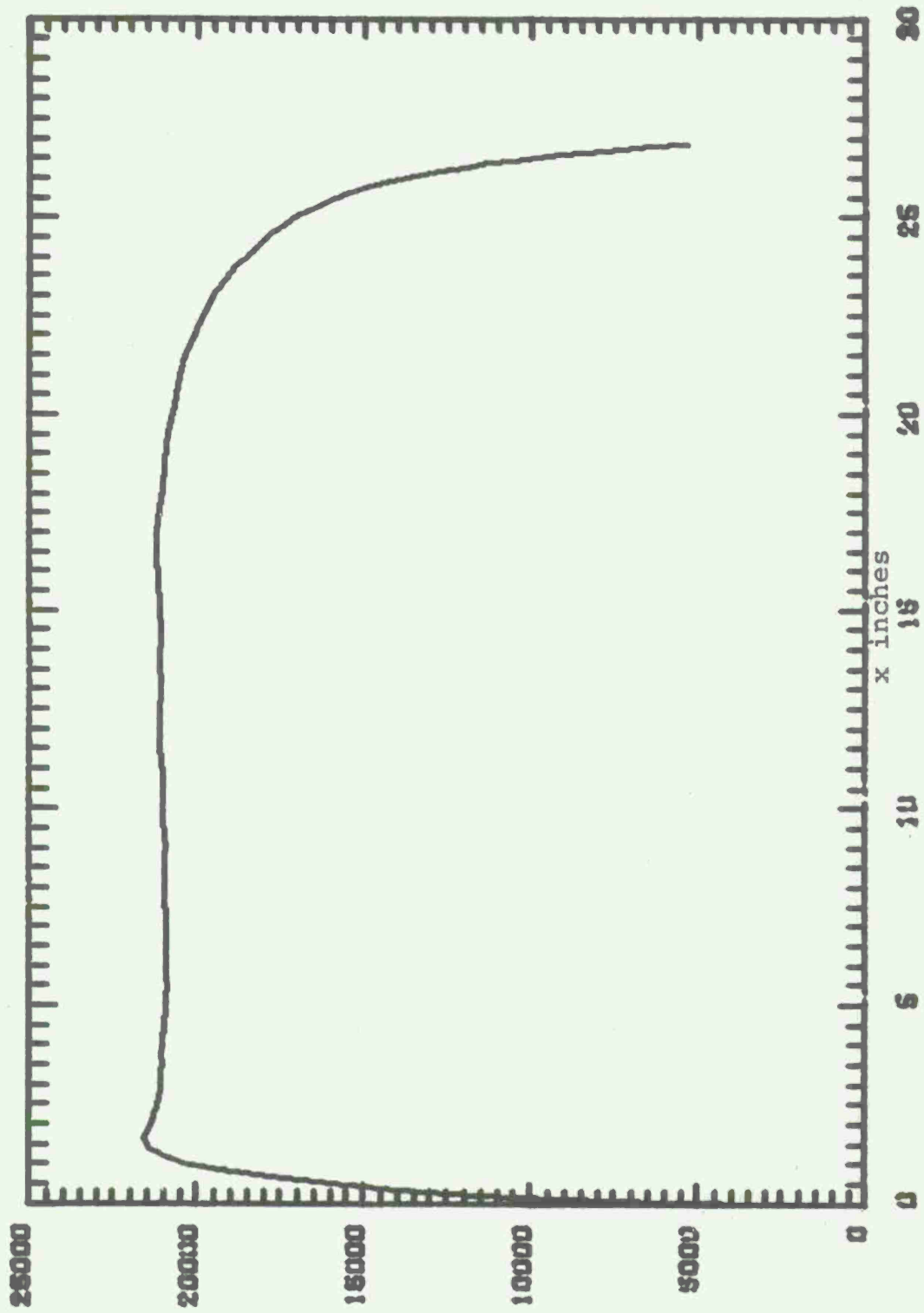


Figure 15 Rod Pull for Zone 7 With No Feedback

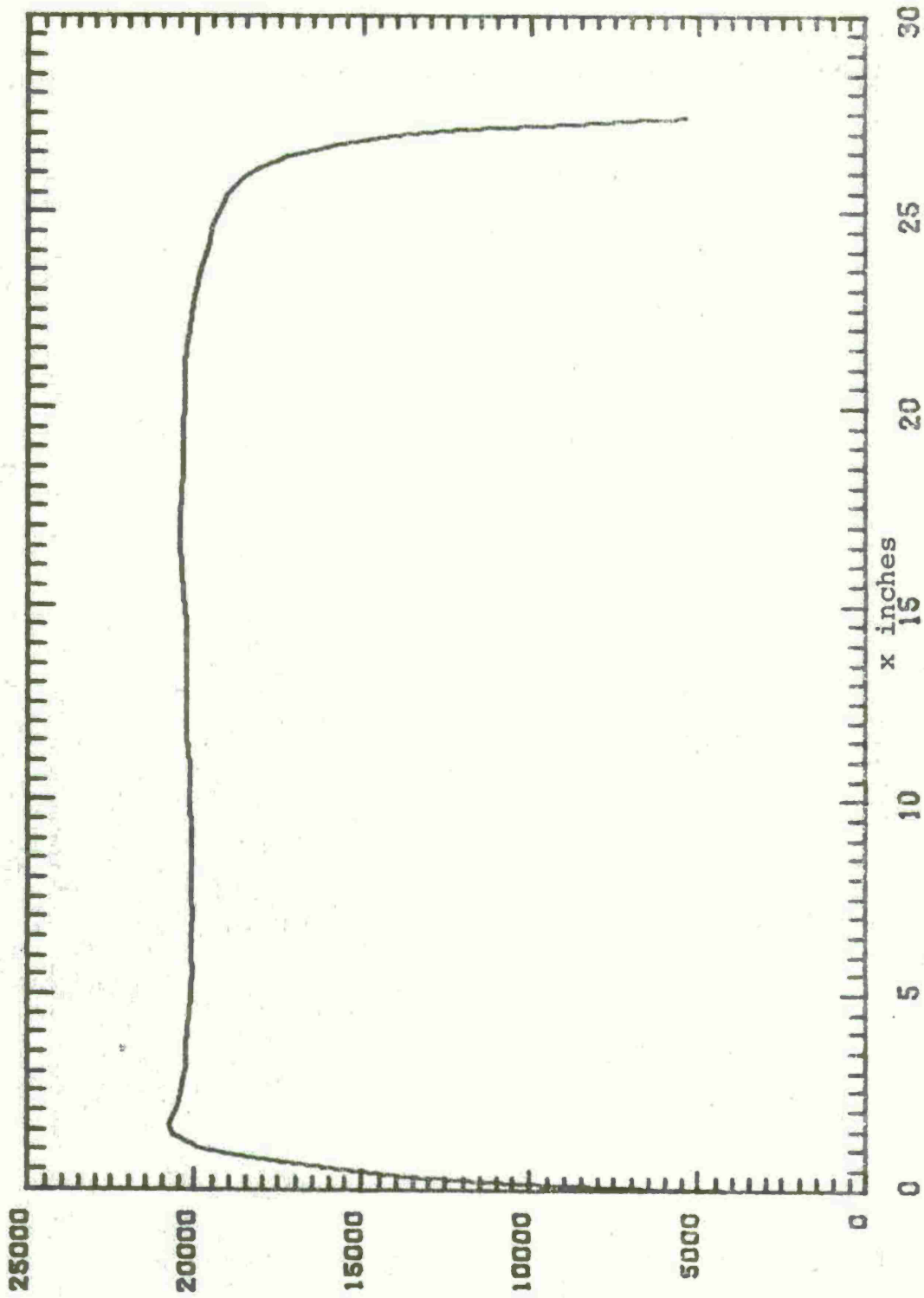


Figure 16 Rod Pull for Zone 7 with Feedback

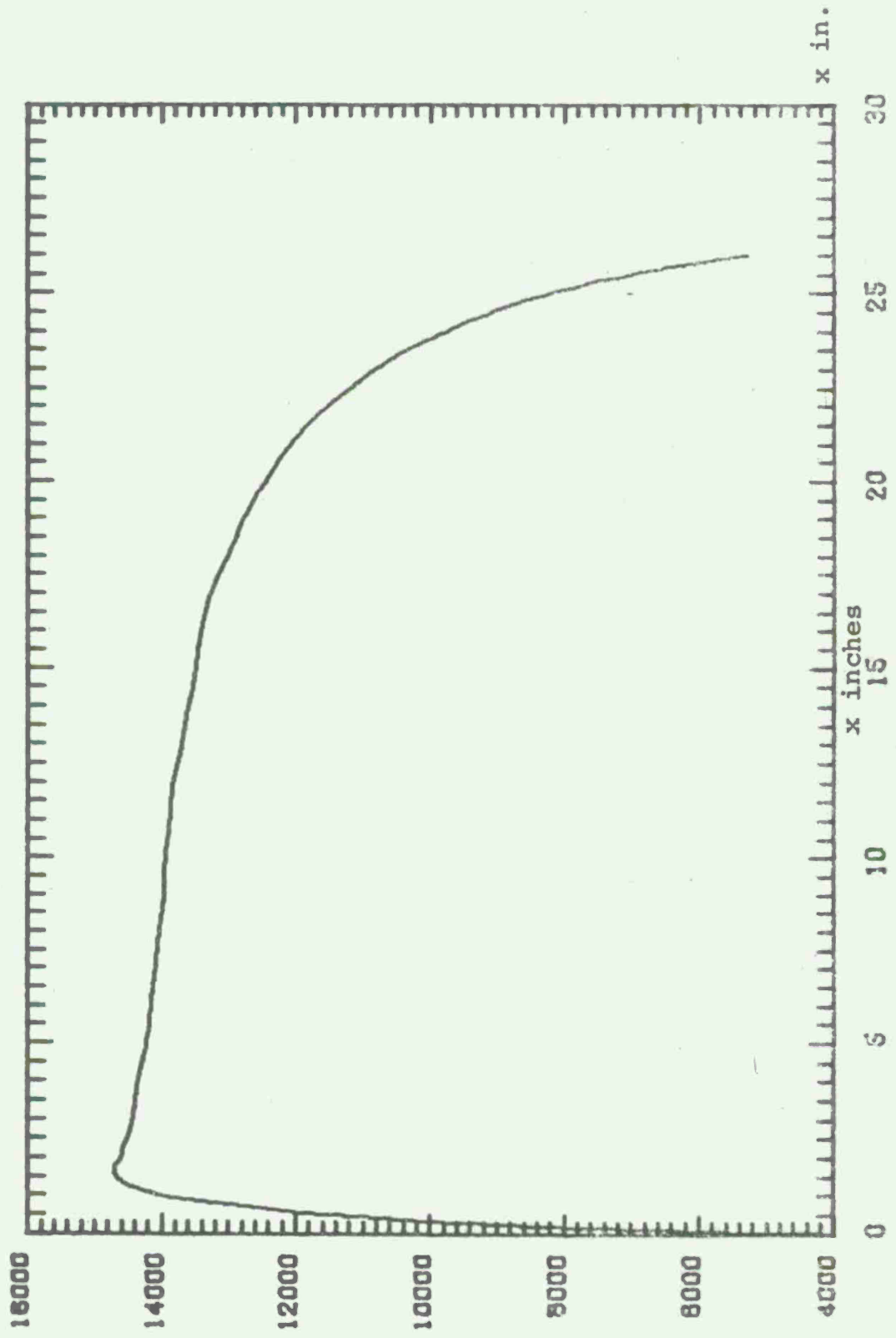


Figure 17 Rod Pull for Zone 6 with No Feedback

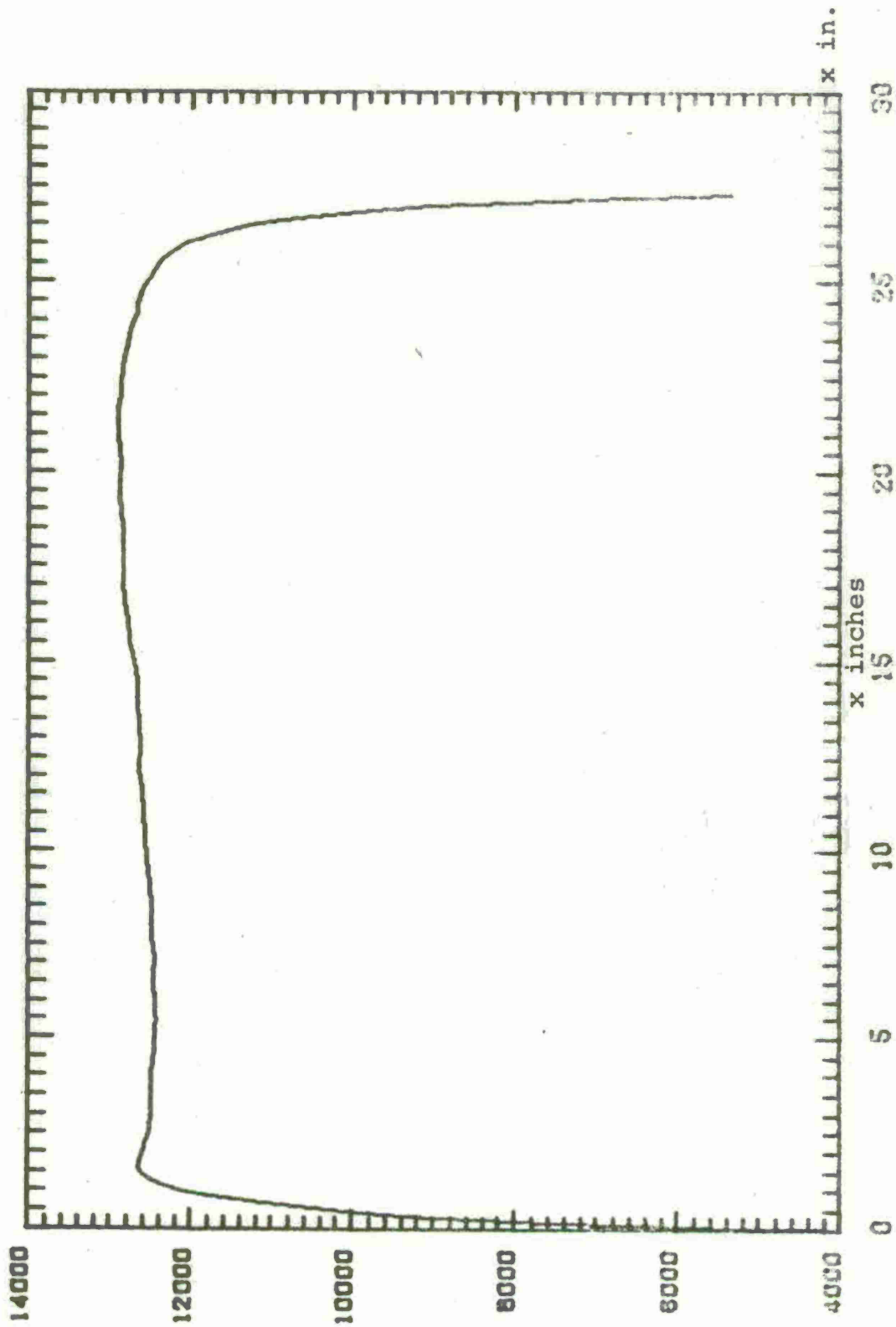


Figure 18 Rod Pull for Zone 6 with Feedback

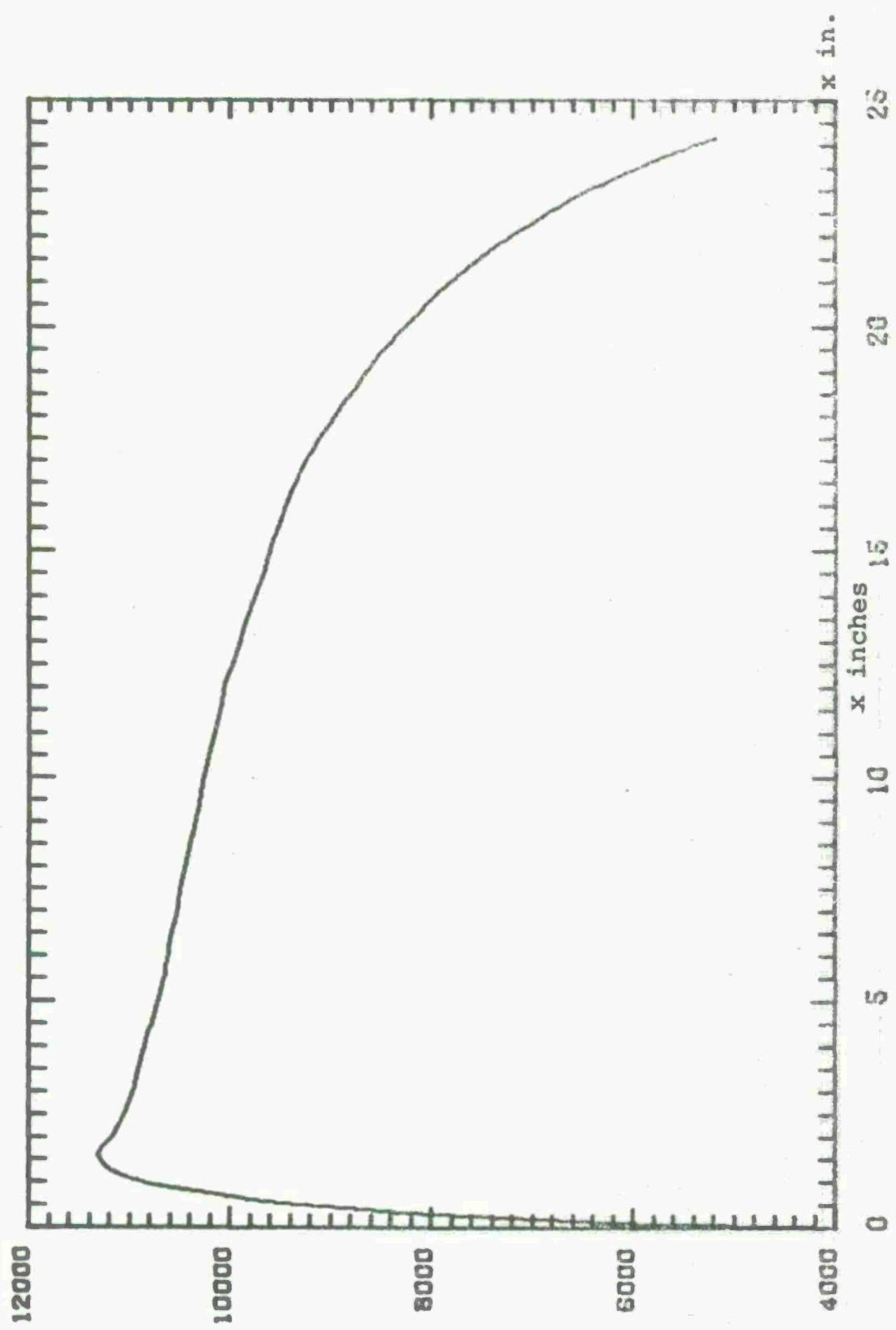


Figure 19 Rod Pull for Zone 5 with No Feedback

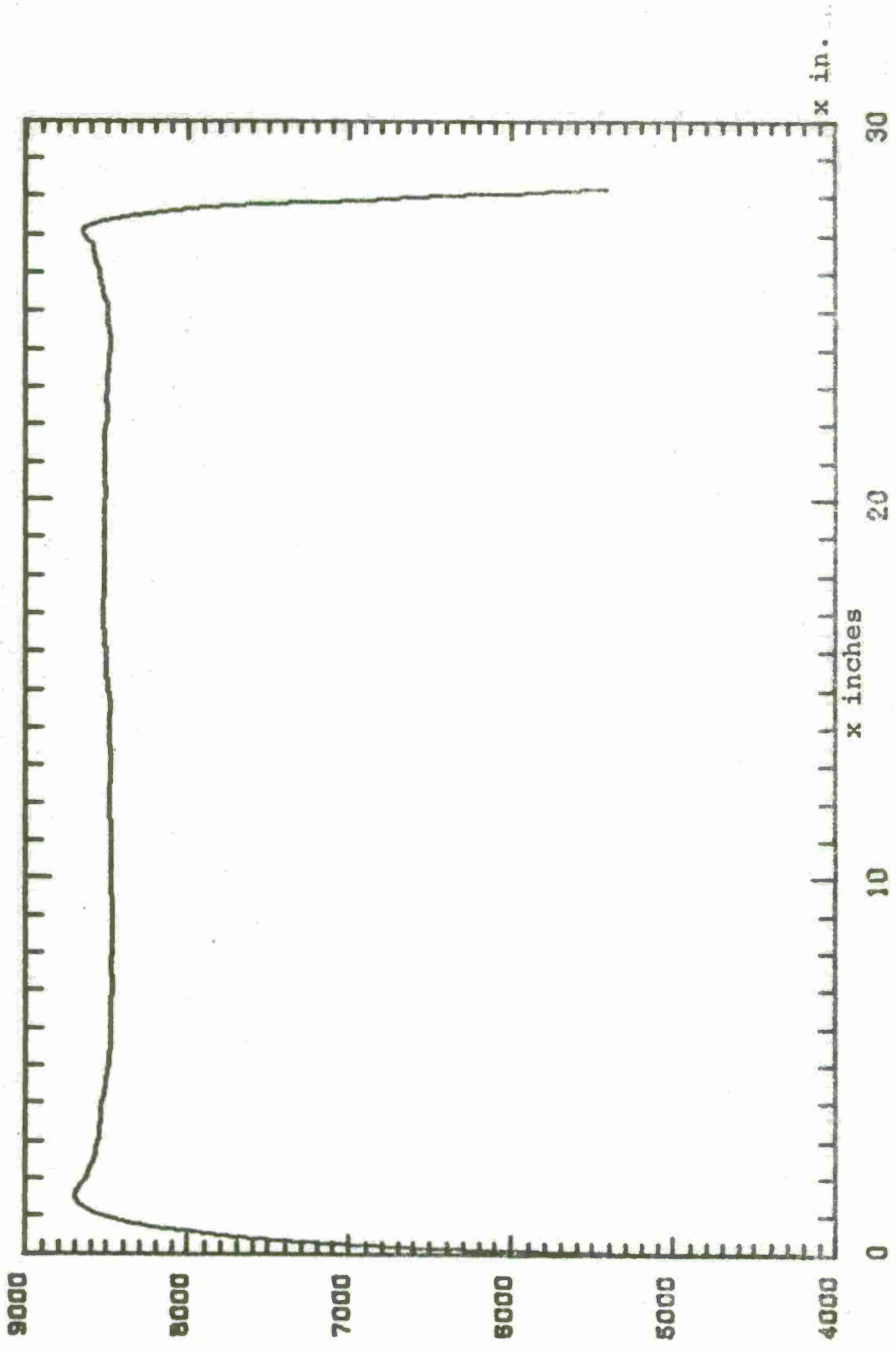


Figure 20 Rod Pull for Zone 5 with Feedback

3.4 Tachometer Feedback

To investigate different control strategies, only velocity feedback of the form $u = g_1 \dot{x}$ was studied. In general, it worked very well for lower zones 6, 5 and 1 but failed to improve the trajectories for zone 7 and made it worse for zone 8. The optimum feedback gain was arrived at by trial and error.

Trajectory for zone 7 with tachometer feedback gain $g_1 = .006E-3$ (Fig. 21) is not much of an improvement over one without feedback (Fig.15). Fig. 22 for zone 6 with $g_1 = .025E-3$ shows a substantial improvement over Fig. 17, the maximum force being 13,200 lbs.; though it is not better than linear state feedback (Fig.18). Fig. 23 for zone 5 with $g_1 = .07E-3$ is trapezoidal and significant reduction in maximum rod pull to 9,400 lbs., but is not better than linear state feedback of Fig. 20. Trajectory for zone 1 with $g_1 = .35E-3$ (Fig. 24) is also very good with reduction to 5,350 lbs. over Fig. 25 (24%).

Non-linear feedback control laws of the form

$$U = g_1 x + g_2 \dot{x} + g_3 x^2 + g_4 \dot{x}^2$$

were investigated for zone 7. The trajectory obtained were with no improvement and sometimes were worse than those with no feedback.

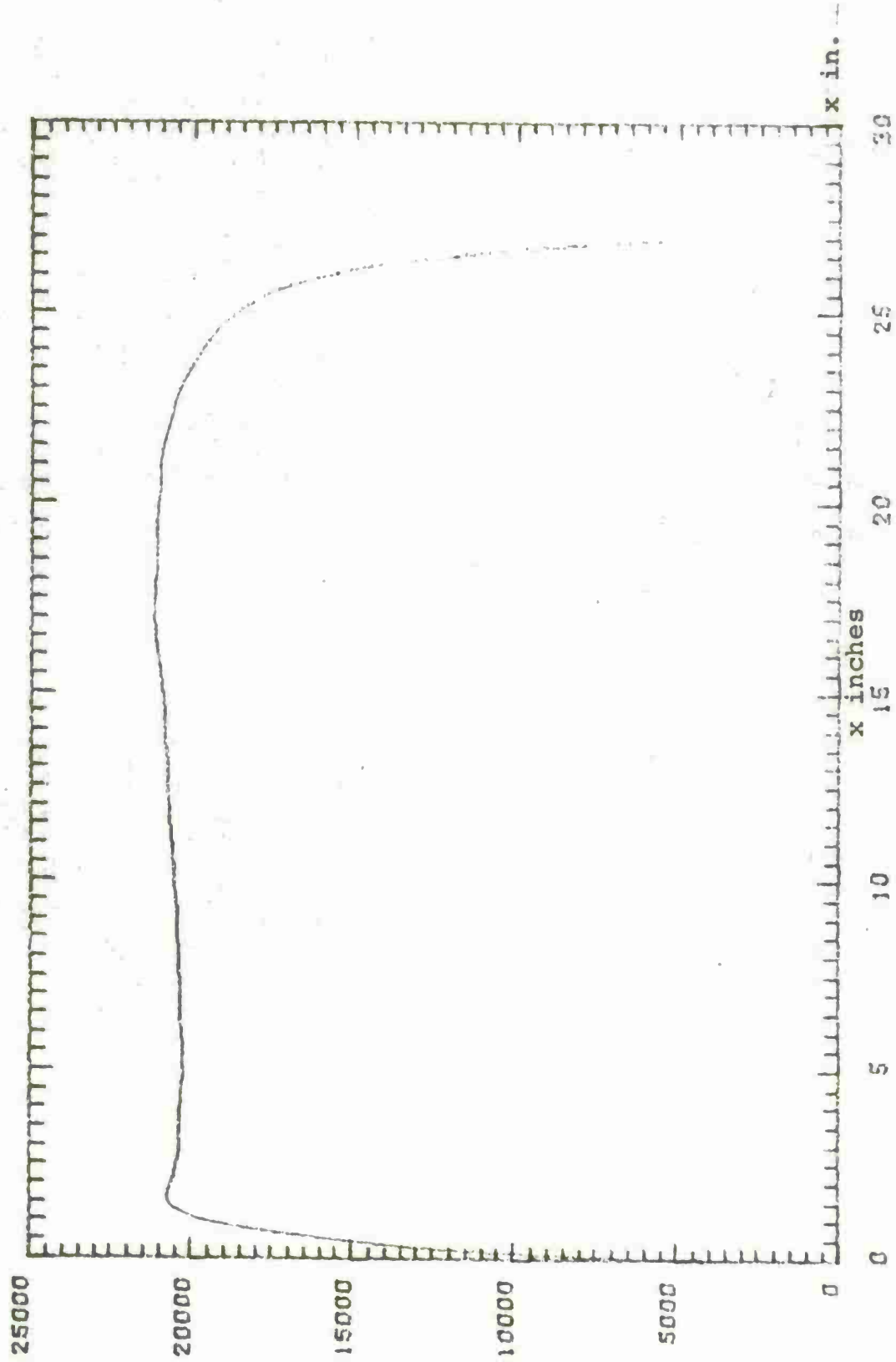


Figure 21 Rod Pull for Zone 7 with Velocity Feedback

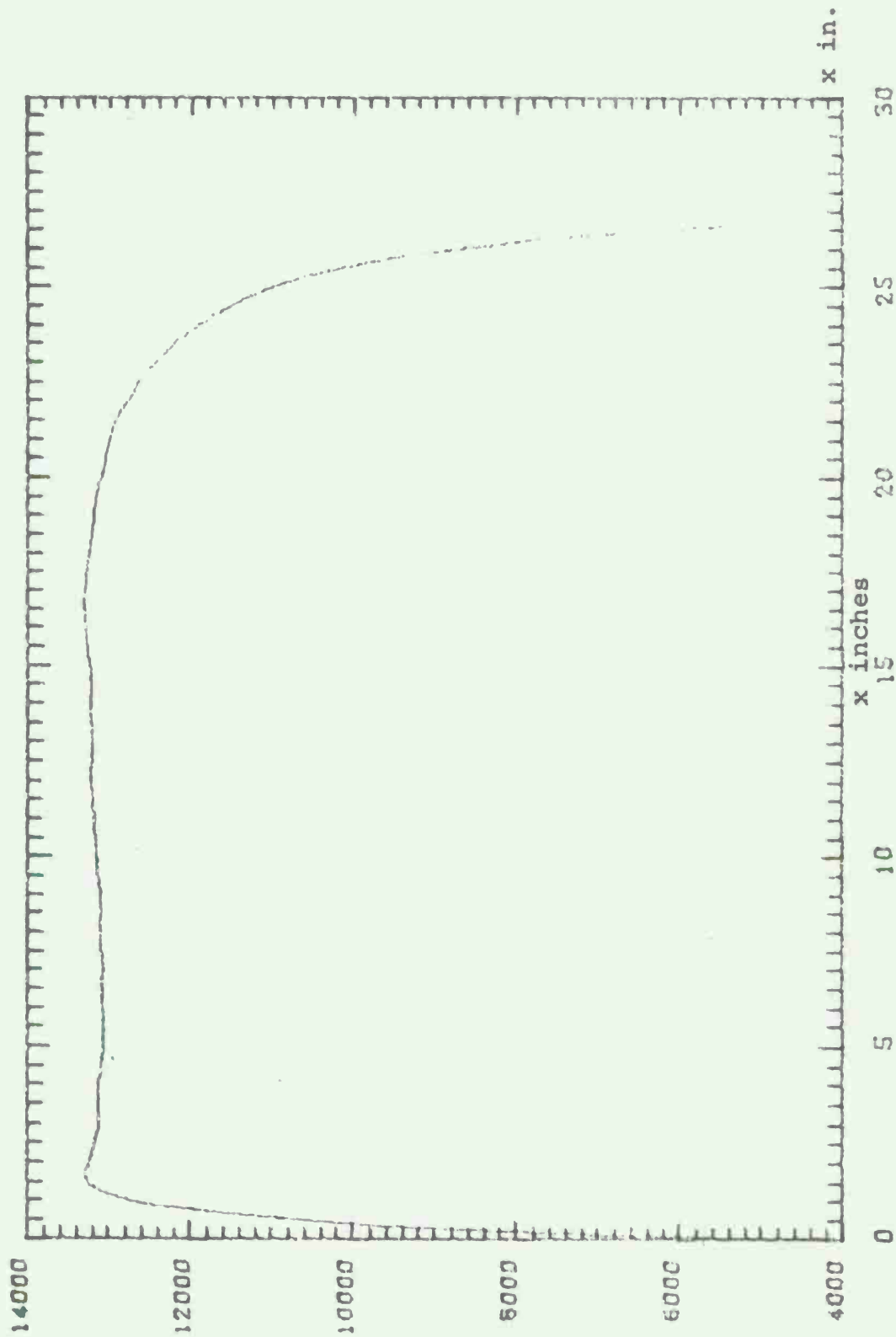


Figure 22 Rod Pull for Zone 6 with Velocity Feedback

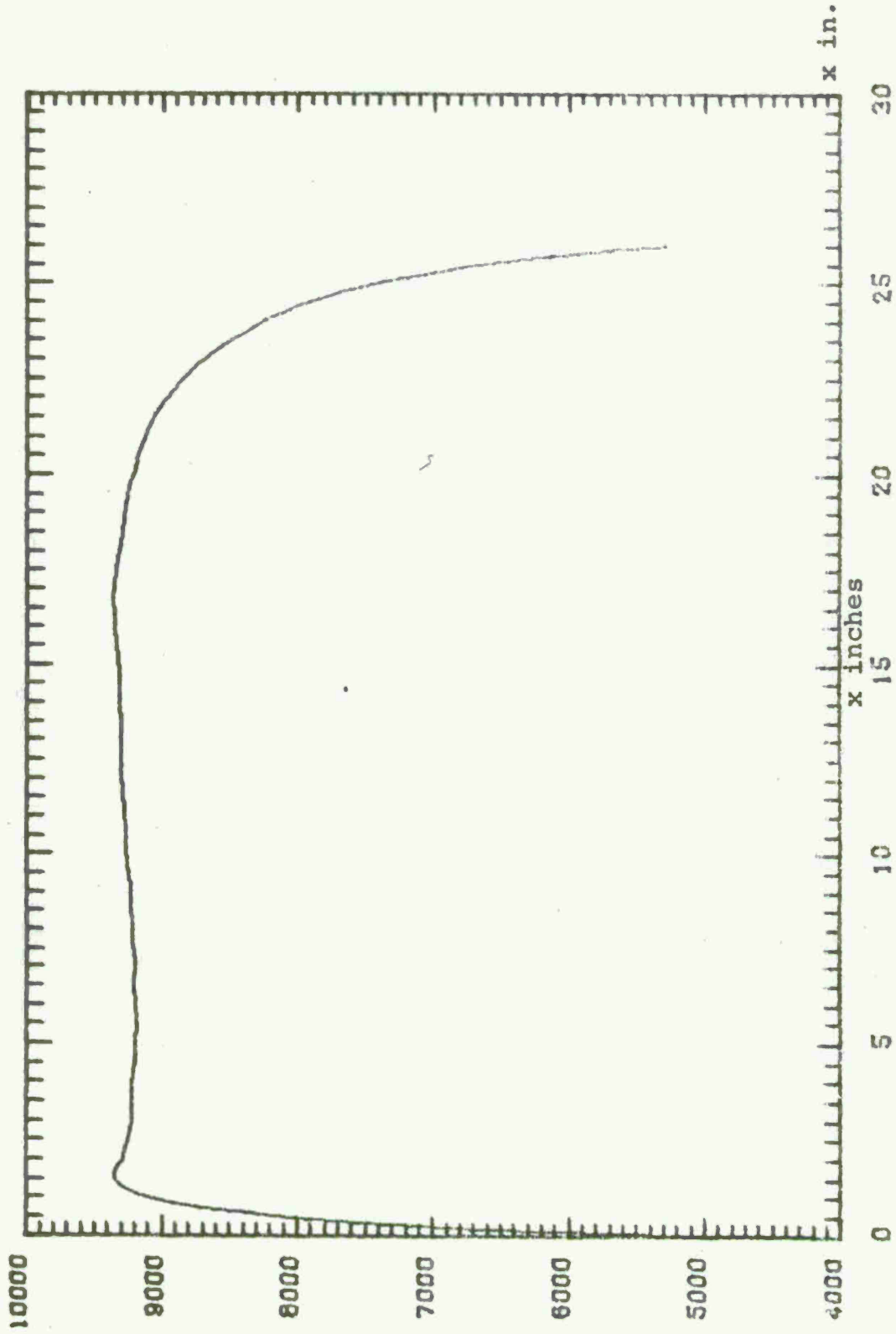


Figure 23 Rod Pull for Zone 5 with Velocity Feedback

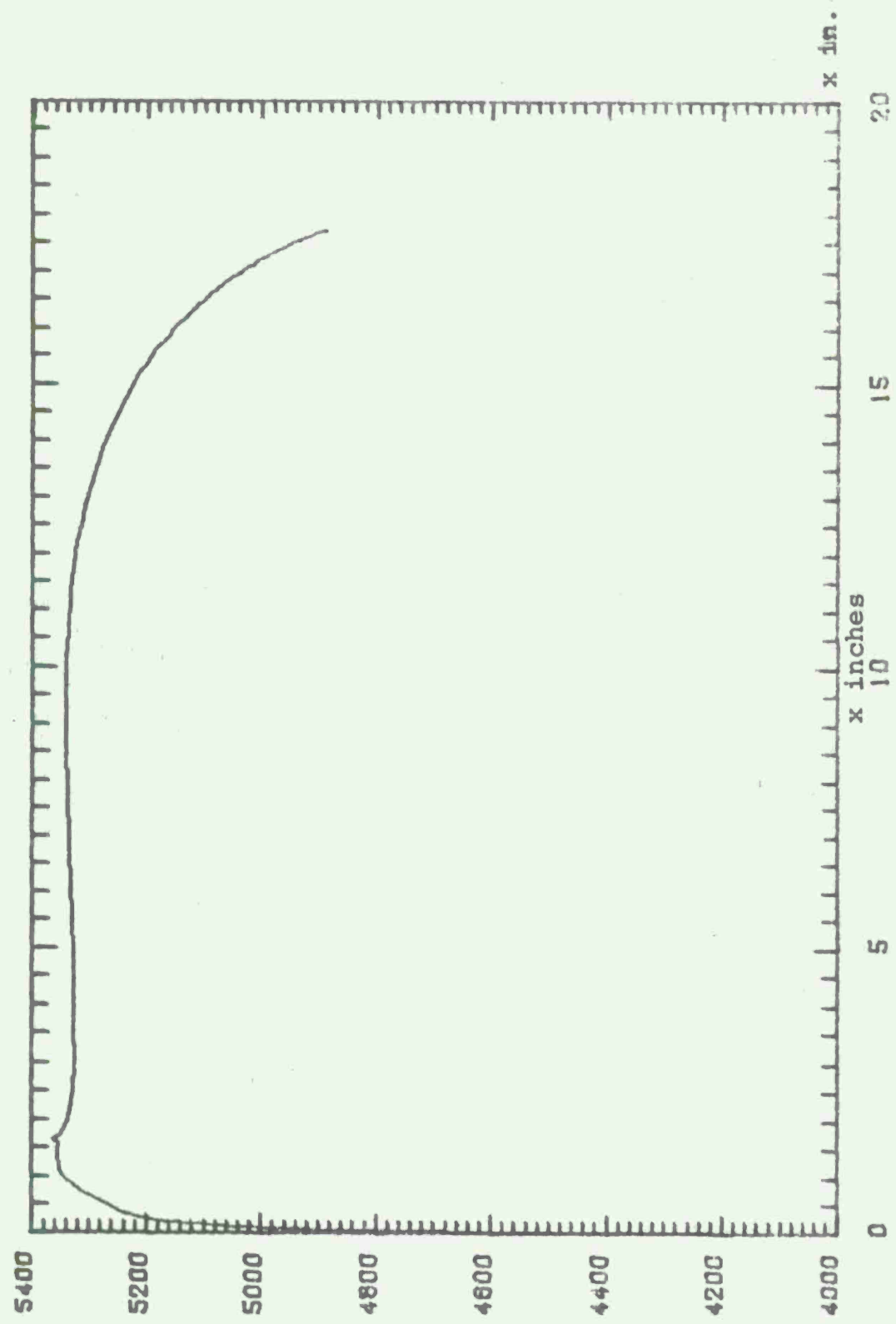


Figure 24 Rod Pull for Zone 1 with Velocity Feedback

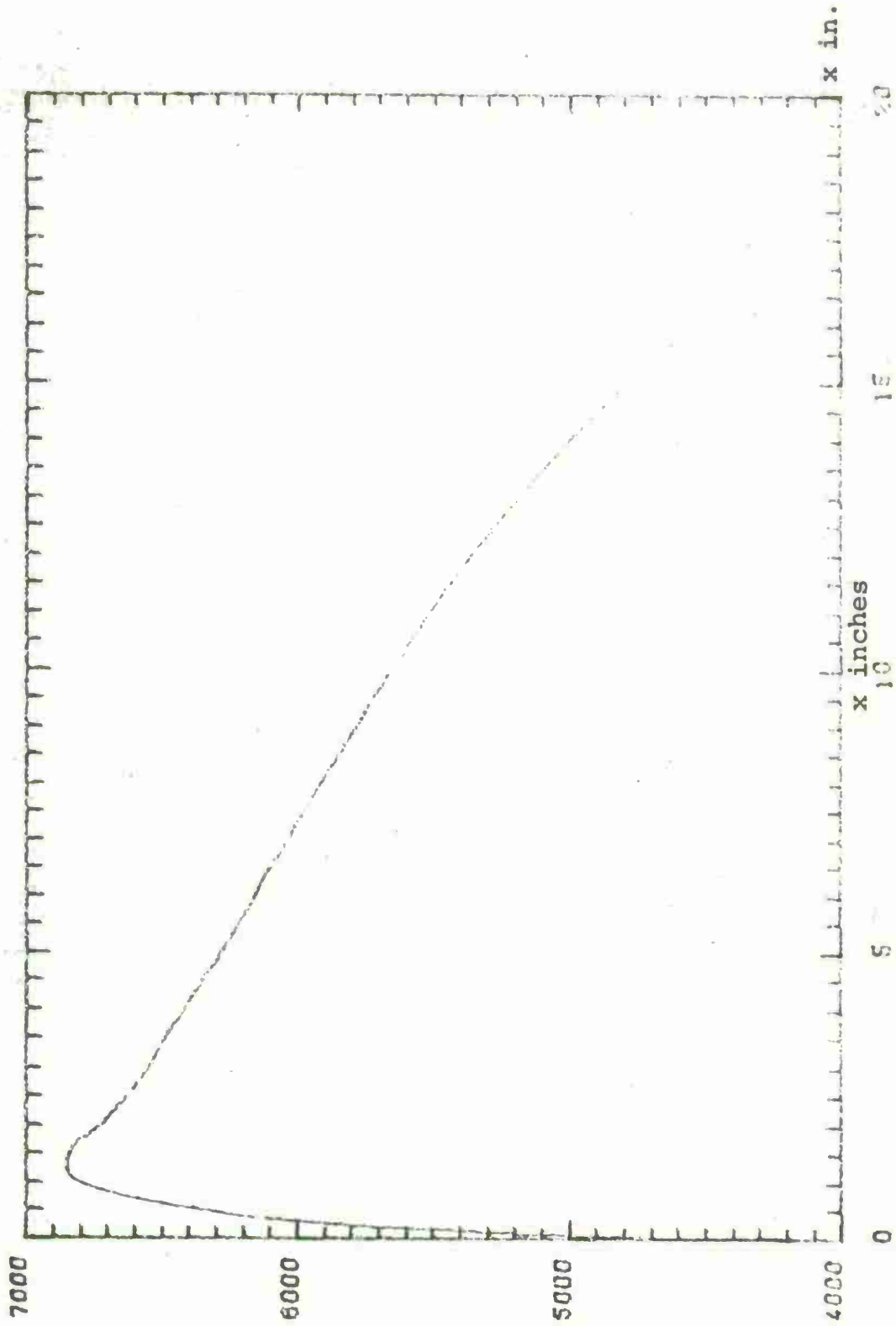


Figure 25 Rod Pull for Zone 1 with No Feedback

CONCLUSIONS

A mathematical model for a conventional hydropneumatic recoil mechanism was developed and simulated on a digital computer by method of Phase-Plane-Delta. A linear state feedback control system was proposed which can be implemented by retrofitting the present designs with a servo-valve to operate in tandem with the variable area groove in the floating piston.

An objective function with direct relation to performance and physical constraints of the system was developed. Davidon-Fletcher-Powell nonlinear optimization algorithm was chosen to optimize this objective function. The procedure was applied to M-37. recoil mechanism with reduction in peak recoil forces from 25 to 2.5% for lower zones and cavitation was avoided for zone 8. Tachometer feedback was shown to be effective for low zones.

The concept of feedback control system coupled with optimization procedure to design recoil mechanisms was demonstrated to be an efficient and very effective tool. The flexibility of feedback control is added retaining robustness of design.

The techniques of feedback control and optimization procedures are recommended for design of counter recoil and other design problems in recoil mechanism.

REFERENCES

1. Seireg, Ali, Mechanical Systems Analysis, International Textbook Company, 1969.
2. Gottfried, Byron S. and Weisman, Joel, Introduction to Optimization, Prentice-Hall Inc., Englewood Cliffs, New Jersey, 1973.
3. Walsh, G.R., Methods of Optimization, John Wiley & Sons, New York, 1975.
4. Bellman, Richard, Mathematical Optimization Techniques, University of California Press, Berkley, 1963.
5. Adby, P.R., and Dempster, M.A.H., Introduction to Optimization Methods, Chapman and Hall, London, 1974.
6. Box, M.J., "A New Method of Constrained Optimization and a Comparison With Other Methods," The Computer Journal, 8, pp. 42-52, 1975.
7. Box, M.J., "A Comparison of Several Current Optimization Methods and the Use of Transformations in Constrained Optimization," The Computer Journal, 9, pp. 67-77, 1966.
8. Nerdahl, M.C. and Frantz, J.W., "Development of a Mathematical Model for Designing Functional Controls of a Soft-Recoil Mechanism," Army Weapons Command, Rock Island, Illinois, AD 713565.
9. Nerdahl, M.C. and Frantz, J.W., "Engineering Analysis, Recoil Mechanisms, XM45 Design of Control Grooves and Prediction of System Motion," Army Weapons Command, Rock Island, Ill. Research and Engineering Directorate, AD-876 531L, October 1970.
10. Frantz, J.W. and Nerdahl, M.C., "Mathematical Models for Engineering Analysis and Design of Howitzer, Medium, Towed, 155 mm, XM198," Artillery Systems Laboratory, Research and Engineering Directorate, U.S. Army Weapons Command, Rock Island, Ill., AD-876775L, October 1970.

Appendix I

Phase-plane-delta simulation of non-linear systems

Phase-plane-delta method is an efficient and fast simulation method for non-linear second order differential equations. A generalized phase plane method is also suitable for higher order non-linear differential models; for details see "Mechanical Systems Analysis" by A. Seireg [1]. The procedure is discussed below for second order equation reproduced with some variation from Prof. Seireg's book.

Consider a linear homogeneous second order differential equation

$$\ddot{x} + \omega_n^2 x = 0 \quad (1)$$

The solution to this equation being

$$x = A \sin (\omega_n t + \phi) \quad (2)$$

$$\dot{x} = A\omega_n \cos (\omega_n t + \phi) \quad (3)$$

From equation 2 and 3, it can be seen that

$$x^2 + \left(\frac{\dot{x}}{\omega_n}\right)^2 = A^2$$

which represents a circle in the x versus $\frac{\dot{x}}{\omega_n}$ plane. This type of plot is known as the phase plane and is a very powerful and useful tool in the analysis of dynamic problems. It could be seen from Fig.26 that the horizontal projection of the motion on a time scale will give the velocity curve plotted to a scale ω_n . The

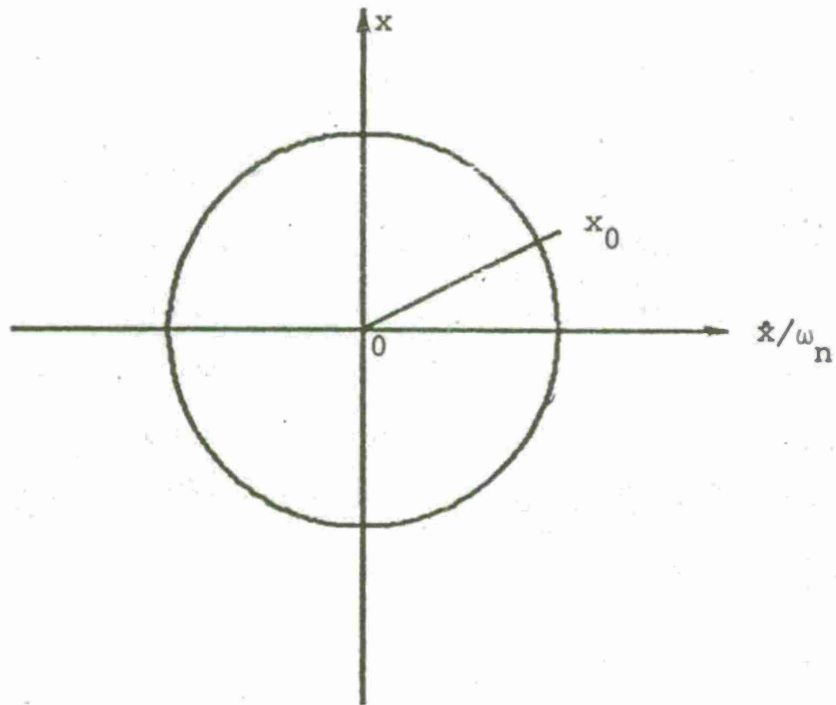


Figure 26 Phase Plane Method

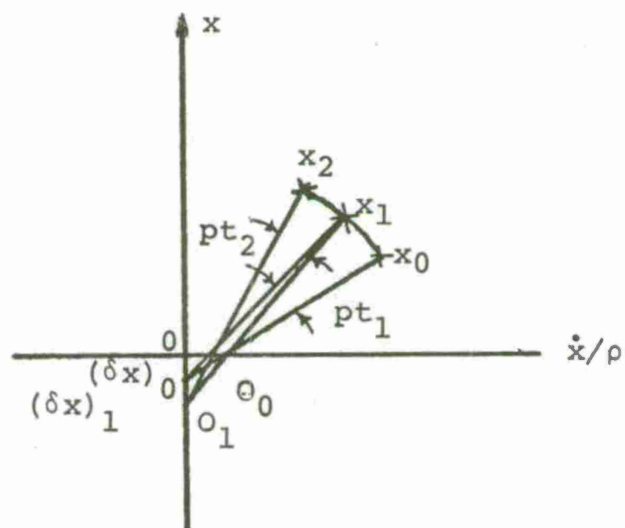


Figure 27 Phase Plane Delta Method

starting point X_0 on the circle is defined by initial conditions at $t = 0$, say $x = x_0$ and $\dot{x} = \dot{x}_0$; the amplitude of motion being

$$A = \sqrt{x_0^2 + (\dot{x}_0/w_n)^2}$$

The complete procedure is detailed step by step as follows

- 1) Calculate the natural frequency w_n of the system
- 2) Plot the two perpendicular axes representing x and (\dot{x}/w_n) respectively. These two axes represent the phase plane.
- 3) The origin O of the phase plane represents the equilibrium condition of the system.
- 4) Knowing the initial conditions of the motion in terms of initial displacement and velocity, a point X_0 can be plotted in the phase plane.
- 5) The free vibration of the system is represented by a circle. The center of the circle is the equilibrium point O . The radius of the circle is the distance OX_0 joining the origin to the initial point X_0 .
- 6) The conditions of motion at any time t_1 are represented by the coordinates of the point X_1 on the circle at a radial angle $w_n t_1$ from X_0 in the counterclockwise direction.

- 7) The projection of the phase-plane plot on a time scale in the direction of x , $(\frac{\dot{x}}{w_n})$ gives the displacement and velocity functions respectively.
- 8) All information concerning the time history of the motion can be obtained from the phase-plane plot.

This scheme can be implemented on a digital computer

The phase-plane-delta method

The phase plane method previously discussed is used to study free vibrations of a linear system. With a slight modification, phase-plane method can be used for forced non-linear vibration problems as follows.

Let the system be

$$m\ddot{x} + k f(x, \dot{x}, t) - F(t) = 0 \quad (4)$$

Rewriting the equation

$$\ddot{x} + \frac{k}{m} [f(x, \dot{x}, t) - x - F(t)/k] = 0$$

or

$$\ddot{x} + p^2 [x + \delta x] = 0 \quad (5)$$

where $\delta x = [f(x, \dot{x}, t) - x - F(t)/k]$ & $p = \sqrt{k/m}$

and is a known function of x , \dot{x} , t , $F(t)$. Equation 5 takes the same form as equation 1 where p^2 takes the place of w_n^2 and x has to be continually modified by an amount δx which is a function x , \dot{x} , t , and $F(t)$.

Therefore, at any instant of time the nonlinear equation can be represented in the phase-plane as a free vibration of a linear system with a continually changing datum.

The procedure is outlined step by step as follows.

- 1) Write the equation in the form

$$\ddot{x} + p^2 (x + \delta x) = 0$$

where p^2 is a constant.

- 2) Express δx as a function $x, \dot{x}, t, F(t)$.
- 3) Plot the phase plane axes to represent $x, (\dot{x}/p)$
Fig. 27.
- 4) Knowing initial conditions x_0, \dot{x}_0 , a point X_0 can be plotted in the phase plane.
- 5) The value of $(\delta x)_0$ is also calculated for the initial condition at time $t = t_0$.
- 6) The center O_0 of the instantaneous linear vibration at the initial phase of the motion is therefore located on the x -axis at a distance $(\delta x)_0$ from the origin. When δ is positive, the distance is taken on the negative x -axis and vice-versa.
- 7) The instantaneous free vibration at the initial phase of the motion can be represented by a small arc of a circle with center O_0 and radius O_0X_0 in the counter-clockwise direction.
- 8) A new condition X_1 is reached after a small increment of time t_1 where the displacement x_1 and the velocity is \dot{x}_1 .

- 9) The value of $(\delta x)_1$ corresponding to this new condition can be calculated, and a new center of oscillation O_1 is determined.
- 10) The new condition X_2 corresponding to an additional increment of time t_2 can be obtained from the arc of a circle with center O_1 , having a radius $O_1 X_1$ and subtending an angle pt_2 in the counterclockwise direction.
- 11) This procedure is then repeated until the time required is reached.
- 12) It should be noted here that the accuracy of this procedure depends on the magnitude of the angular displacement pt . Better accuracy can be attained also by iteration. This means that after X_1 is determined, a value of δx is calculated which corresponds to a point midway between X_0 and X_1 . Using this new value of δx , a better approximation for the new position X_1 after a small increment of time t_1 can be obtained. This procedure can be repeated until a desired accuracy is achieved.
- 13) This procedure is suitable for programming on a high-speed digital computer.

APPENDIX II
ALGORITHMS FOR OPTIMIZATION
OF NON-LINEAR FUNCTIONS

Three algorithms for non-linear optimization are discussed:

- 1) Davidon-Fletcher-Powell unconstrained optimization with cubic interpolation.
- 2) Davidon-Fletcher-Powell unconstrained optimization with linear search by golden section.
- 3) Constrained optimization by Random search.

A short introduction to gradient methods of optimization is presented.

The problem of non-linear optimization can be stated as

Find a vector x of parameters to minimize

$J(x)$, an objective function subject to certain constraint of type

$$C_i(x) \leq, = \text{ or } \geq b_i$$

We can express $J(x)$ in Taylor series expansion as

$$J(x + \Delta x) = J(x) + \Delta x'g + \frac{1}{2} \Delta x' G \Delta x + \dots \quad (1)$$

where Δx is a vector of increment in x

g is the gradient vector

G is the Hessian Matrix of second order partial derivatives

The first order approximation is

$$J(x + \Delta x) = J(x) + \Delta x'g$$

The reduction in the function $J(x)$ for moving to $x+\Delta x$ is $\Delta x'g$ and is maximum if we move in the negative direction of gradient vector g .

$$\therefore \Delta x = -\lambda \frac{g}{|g|} \quad (2)$$

The optimum value of λ is found by univariate linear search in the direction $-\frac{g}{|g|}$.

This is called the steepest descent method. This method converges very slowly. The extension of this method is the conjugate gradient method. Assuming the objective function is quadratic of the form,

$$J(x) = \frac{1}{2} x'Gx + bx + c \quad (3)$$

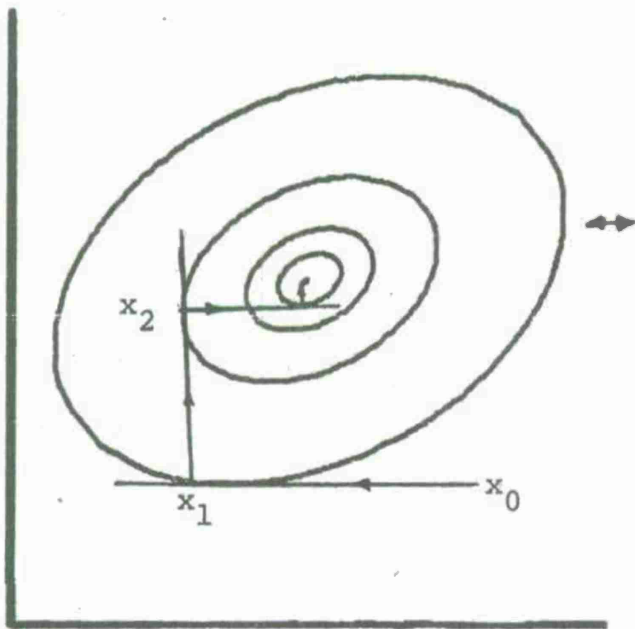
one can find a sequence of search directions u_1, u_2, \dots, u_k such that

$$u_i' Gu_j = 0 \quad i \neq j \quad (4)$$

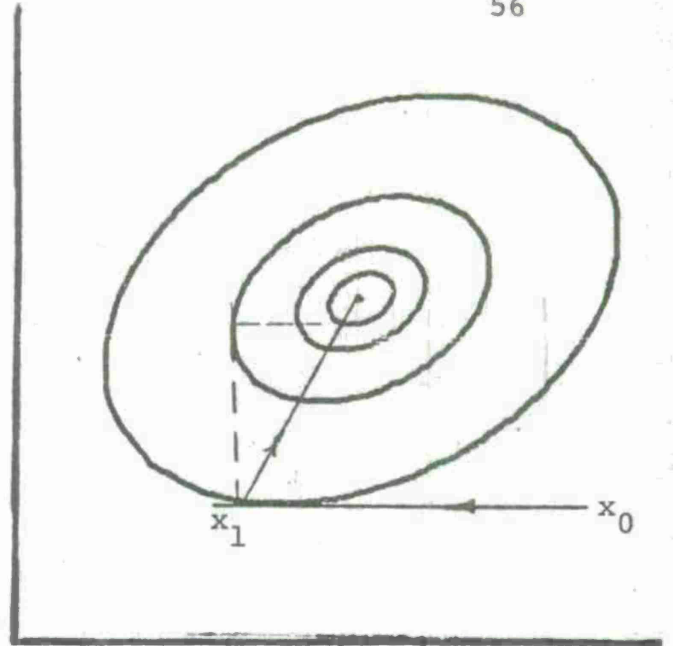
By moving sequentially in the directions u_1, u_2, \dots, u_k with linear univariate searches we can reach the optimum

$$X_{\min}^* = X_0 + \sum_{i=1}^n \lambda_i u_i \quad (5)$$

The steepest descent and conjugate gradients are illustrated in Fig. 28 for two parameter case



Steepest Descent



Conjugate Gradient

Figure 28a

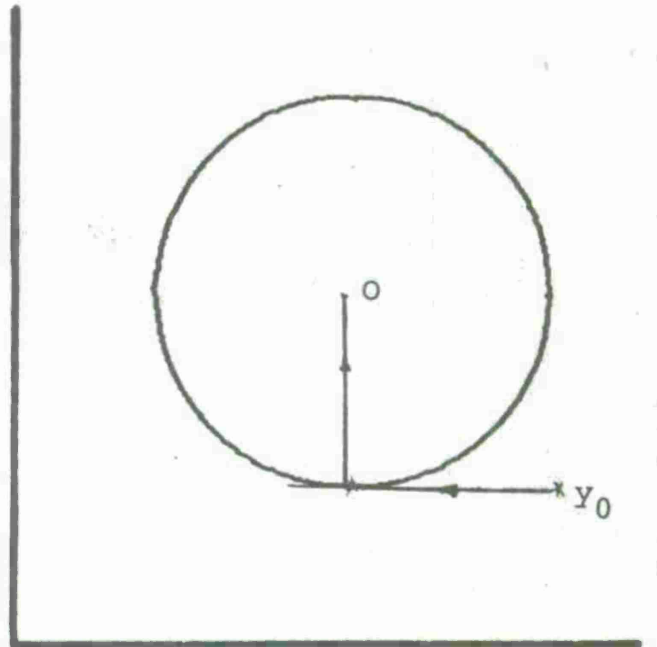
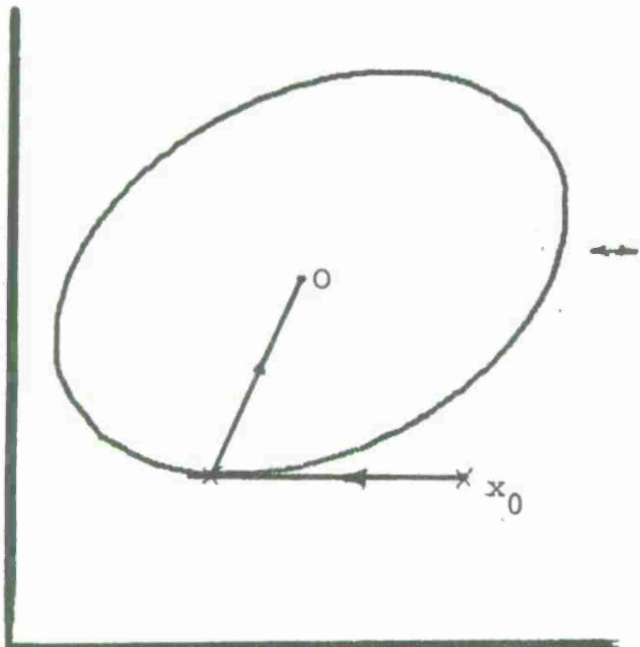


Figure 28b Concept of Conjugate Gradient

The conjugate gradient method transforms concentric elliptic contours into concentric circular contours. The circular contour has the desirable property of the normal to the tangent at any point passes through the center. Once the direction of normal is found in this plane, it can be transformed back to the original plane and direction of the increment in x can be found out and this will pass through the minimum for the quadratic function.

(3) Newton-Raphson Method

$$J(x+\Delta x) = J(x) + \Delta x'g + \frac{1}{2} \Delta x'G \Delta x \quad (6)$$

differentiating with respect to Δx

$$\frac{\partial J(x+\Delta x)}{\partial \Delta x} = g + G\Delta x$$

for $x+\Delta x$ to be a optimum point

$$\frac{\partial J(x+\Delta x)}{\partial \Delta x} = 0$$

$$g + G\Delta x = 0 \quad , \quad \Delta x = -G^{-1}g \quad (7)$$

This method is called Newton-Raphson and is a very efficient method if G and g are available.

The problem for non-quadratic function minimization is to find G which is positive definite and the question of how good an approximation of second order Taylor expansion is. The combination of conjugate gradient method for fast movement when away from minimum can be utilized with the conjugacy being with respect to the Hessian G . The Davidon-Fletcher-Powell (DFP) algorithm does exactly that.

The DFP algorithms continuously updates H , the inverse of the hessian matrix with linear search in direction of conjugate gradient by cubic interpolation. The step by step procedure given below is reproduced with variation from [4]. The details can be found in [2,3,4 & 5].

1) Set $H_1 = I$ and let k be the current iteration number, then set

$$d_k = -H_k g_k \quad (8)$$

then, d_k is the direction of search from the current point x_k

2) Perform a linear search to find $\lambda_k^* (>0)$, where λ_k^* is the value of λ_k that minimizes $J(x_k + \lambda_k d_k)$

$$3) \text{ Set } \Delta x_k = \lambda_k^* d_k \quad (9)$$

$$4) \text{ Set } x_{k+1} = x_k + \Delta x_k \quad (10)$$

giving the new current point

5) Evaluate $J(x_{k+1})$ and g_{k+1}

$$6) \text{ Set } \Delta g_k = g_{k+1} - g_k \quad (11)$$

$$7) H_{k+1} = H_k + \frac{\Delta x_k \Delta x_k'}{\Delta x_k' \Delta g_k} + \frac{H_k \Delta g_k \Delta g_k' H_k}{\Delta g_k' H_k \Delta g_k}$$

8) Set $k=k+1$ and return to step 1.

9) Stop when either $|d_k|$ or every component of d_k is smaller than some prescribed amount.

The linear search in step 2 can be performed in two ways with cubic interpolation or golden section search.

Cubic interpolation procedure:

1) Evaluate $J_0 = J(x_k)$ and $G_0 = g'_k d_k$ (12)

check $G_0 < 0$. Compute α by

$$\alpha = \min\left[2, -\frac{2(J_0 - J_e)}{G_0}\right] \quad (13)$$

where J_e is the estimated values of $J(x_k + \lambda^*_k d_k)$.

2) Evaluate $J_\alpha = J(x_k + \alpha d_k)$ and $G_\alpha = g'_\alpha d_k$

3) If $G_\alpha > 0$ or if $J_\alpha > J_0$, proceed to rule 5 otherwise go to rule 4.

4) Replace α by 2α , return to rule 2.

5) Interpolate in the interval $[0, \alpha]$ for λ^*_k using

$$\frac{\lambda^*_k}{\alpha} = 1 - \frac{G_\alpha + w - Z}{G_\alpha - G_0 + 2w} \quad (14)$$

where

$$w = (z^2 - G_0 G_\alpha)^{1/2} \quad (15)$$

and

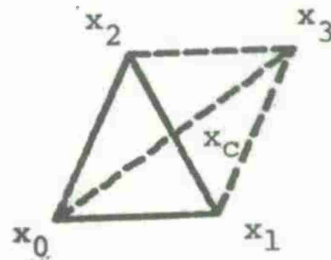
$$Z = \frac{3}{\alpha} (J_0 - J_\alpha) + G_0 + G_\alpha$$

6) Return to rule 5 to repeat the interpolation in the smaller interval $[0, \lambda^*_k]$ or $[\lambda^*_k, \alpha]$ accordingly as

$$g'_{k+1} d_k \geq 0 \text{ or } < 0$$

stop when the interval of interpolation has decreased to some prescribed value.

The complex method of M.J. Box [6], [7], with random search generates a simplex of $n+1$ points where n is the number of parameters to be optimized. The function is computed at each of the vertices and the worst vertex is discarded. The reflection of this discarded vertex into the centroid of the remaining vertices is taken as a new vertex and search is carried out in two dimensions, the procedure is as follows:



Three initial vertices are x_0, x_1, x_2 . Let x_0 be the worst vertex and x_c be the centroid of x_1 and x_2 . Then x_3 is computed by the relation

$$x_3 = (1+\alpha)x_c - \alpha x_{\min}$$

where x_{\min} is vertex with minimum function value. The procedure is repeated until minimum is obtained.

Appendix III

Design Data for M-37 Recoil Mechanism

M-37. recoil mechanism is designed for firing zone 7. All the pertinent parameters necessary for simulation of recoil mechanism model developed in Chapter 1 are given below. The variable area of the groove machined in the floating piston is tabulated in Table 2. Breech forces are tabulated in Tables 3 through 7 for zones 1, 5 through 8. These breech forces are simulated breech force data rather than actual test data. All the design data listed here was provided by Control and Stabilization group of General Rodman Laboratory, Army Weapons Command at Rock Island, Illinois.

$$m_R - \text{Mass of recoiling parts} = 3.6658 \text{ lbf sec}^2/\text{in}$$

$$m_P - \text{Mass of floating piston} = .06735 \text{ lbf sec}^2/\text{in}$$

$$\rho - \text{Mass density of hydraulic fluid} = .78E-4$$

$$P_0 - \text{Initial gas pressure} = 1153 \text{ psi}$$

$$V_0 - \text{Initial volume of gas} = 513 \text{ in}^3$$

$$R - \text{Gas constant} = 1.68$$

$$A_R - \text{Recoil piston area} = 2.9906 \text{ in}^2$$

$$A_C - \text{Control rod area} = 2.4053 \text{ in}^2$$

$$A_D - \text{Floating piston area} = 11.781 \text{ in}^2$$

$$C_1=C_2=C_3 - \text{Discharge coefficients} = .8$$

$$A_1 - \text{Area of orifice 1} = 1.25 \text{ in}^2$$

$$A_2 - \text{Area of orifice 2} = .4536 \text{ in}^2$$

TABLE 2- AREA OF VARIABLE ORIFICE A3

| X | A3(X) | X | A3(X) |
|----------|--------|----------|---------|
| 0.00000 | .08680 | 15.12600 | .07900 |
| .50420 | .09370 | 15.63020 | .07710 |
| 1.00840 | .09410 | 16.13440 | .07520 |
| 1.51260 | .09630 | 16.63860 | .07320 |
| 2.01680 | .09950 | 17.14280 | .07130 |
| 2.52100 | .10110 | 17.64700 | .06940 |
| 3.02520 | .10210 | 18.15120 | .06750 |
| 3.52940 | .10250 | 18.65540 | .06540 |
| 4.03360 | .10270 | 19.15960 | .06320 |
| 4.53780 | .10290 | 19.66380 | .06100 |
| 5.04200 | .10280 | 20.16800 | .05880 |
| 5.54620 | .10250 | 20.67220 | .05630 |
| 6.05040 | .10190 | 21.17640 | .05380 |
| 6.55460 | .10120 | 21.68060 | .05120 |
| 7.05880 | .10060 | 22.18480 | .04870 |
| 7.56300 | .09960 | 22.68900 | .04580 |
| 8.06720 | .09870 | 23.19320 | .04290 |
| 8.57140 | .09770 | 23.69740 | .03980 |
| 9.07560 | .09670 | 24.20160 | .03650 |
| 9.57980 | .09540 | 24.70580 | .03270 |
| 10.08400 | .09410 | 25.21000 | .02870 |
| 10.58820 | .09290 | 25.71420 | .02410 |
| 11.09240 | .09150 | 26.21840 | .01910 |
| 11.59660 | .09000 | 26.72260 | .01330 |
| 12.10080 | .08850 | 27.22680 | .00620 |
| 12.60500 | .08720 | 27.73100 | 0.00000 |
| 13.10920 | .08570 | 28.23520 | 0.00000 |
| 13.61340 | .08410 | 28.73940 | 0.00000 |
| 14.11760 | .08250 | 29.24360 | 0.00000 |
| 14.62180 | .08090 | | |

TABLE 3- BREACH FORCE FOR ZONE 1

| T | B(T) | T | B(T) |
|--------|----------|--------|--------|
| .00000 | 9.0 | .03800 | 1757.0 |
| .00050 | 5.0 | .04000 | 1526.0 |
| .00100 | 6.0 | .04200 | 1329.0 |
| .00150 | 7.0 | .04400 | 1159.0 |
| .00200 | 8.0 | .04600 | 1013.0 |
| .00250 | 9.0 | .04800 | 887.0 |
| .00300 | 10.0 | .05000 | 778.0 |
| .00350 | 11.0 | .05200 | 683.0 |
| .00400 | 12.0 | .05400 | 602.0 |
| .00450 | 10.0 | .05600 | 530.0 |
| .00500 | 72.0 | .05800 | 468.0 |
| .00550 | 1177.0 | .06000 | 414.0 |
| .00600 | 2041.0 | .06200 | 367.0 |
| .00650 | 3287.0 | .06400 | 326.0 |
| .00700 | 5272.0 | .06600 | 289.0 |
| .00750 | 8393.0 | .06800 | 257.0 |
| .00800 | 13220.0 | .07000 | 229.0 |
| .00850 | 20477.0 | .07200 | 205.0 |
| .00900 | 30924.0 | .07400 | 183.0 |
| .00950 | 44999.0 | .07600 | 163.0 |
| .01000 | 62189.0 | .07800 | 146.0 |
| .01050 | 80403.0 | .08000 | 131.0 |
| .01100 | 96098.0 | .08200 | 118.0 |
| .01150 | 105714.0 | .08400 | 106.0 |
| .01187 | 107588.0 | .08600 | 95.0 |
| .01250 | 102620.0 | .08800 | 86.0 |
| .01300 | 93260.0 | .09000 | 77.0 |
| .01350 | 82047.0 | .09200 | 70.0 |
| .01400 | 70792.0 | .09400 | 63.0 |
| .01450 | 60482.0 | .09600 | 57.0 |
| .01500 | 51500.0 | .09800 | 52.0 |
| .01550 | 43889.0 | .10000 | 47.0 |
| .01600 | 37532.0 | .10200 | 43.0 |
| .01650 | 32252.0 | .10400 | 39.0 |
| .01700 | 27872.0 | .10600 | 35.0 |
| .01750 | 24231.0 | .10800 | 32.0 |
| .01800 | 21192.0 | .11000 | 29.0 |
| .01850 | 18643.0 | .11200 | 27.0 |
| .01900 | 16493.0 | .11400 | 24.0 |
| .01950 | 14669.0 | .11600 | 22.0 |
| .02000 | 13113.0 | .11800 | 20.0 |
| .02050 | 11778.0 | .12000 | 19.0 |
| .02100 | 10626.0 | .12200 | 17.0 |
| .02150 | 9626.0 | .12400 | 16.0 |
| .02200 | 8755.0 | .12600 | 14.0 |
| .02250 | 7992.0 | .12800 | 13.0 |
| .02300 | 7320.0 | .13000 | 12.0 |
| .02350 | 6726.0 | .13200 | 11.0 |
| .02400 | 6199.0 | .13400 | 10.0 |
| .02450 | 5729.0 | .13600 | 9.0 |
| .02500 | 5309.0 | .13800 | 9.0 |
| .02550 | 4933.0 | .14000 | 8.0 |
| .02600 | 4593.0 | .14200 | 7.0 |
| .02650 | 4286.0 | .14400 | 7.0 |
| .02700 | 4009.0 | .14600 | 6.0 |
| .02724 | 3884.0 | .14800 | 6.0 |
| .02750 | 3803.0 | .15000 | 5.0 |
| .02800 | 3665.0 | .15200 | 5.0 |
| .03000 | 3149.0 | .20000 | 0.0 |
| .03200 | 2712.0 | | |
| .03400 | 2342.0 | | |
| .03600 | 2026.0 | | |

TABLE 4- BREACH FORCE FOR ZONE 5

| T | B(T) | T | B(T) |
|---------|----------|--------|--------|
| 0.00000 | 159.0 | .03600 | 2426.0 |
| .00050 | 246.0 | .03800 | 2069.0 |
| .00100 | 513.0 | .04000 | 1769.0 |
| .00150 | 938.0 | .04200 | 1517.0 |
| .00200 | 1724.0 | .04400 | 1304.0 |
| .00250 | 3118.0 | .04600 | 1123.0 |
| .00300 | 5642.0 | .04800 | 969.0 |
| .00350 | 10127.0 | .05000 | 839.0 |
| .00400 | 18001.0 | .05200 | 727.0 |
| .00450 | 31434.0 | .05400 | 632.0 |
| .00500 | 53257.0 | .05600 | 550.0 |
| .00500 | 85873.0 | .05800 | 480.0 |
| .00600 | 128386.0 | .06000 | 419.0 |
| .00650 | 173036.0 | .06200 | 367.0 |
| .00700 | 206142.0 | .06400 | 322.0 |
| .00748 | 217035.0 | .06600 | 283.0 |
| .00750 | 217008.0 | .06800 | 249.0 |
| .00800 | 205962.0 | .07000 | 220.0 |
| .00850 | 181687.0 | .07200 | 194.0 |
| .00900 | 153385.0 | .07400 | 172.0 |
| .00950 | 126693.0 | .07600 | 152.0 |
| .01000 | 103872.0 | .07800 | 135.0 |
| .01050 | 85258.0 | .08000 | 120.0 |
| .01100 | 70386.0 | .08200 | 107.0 |
| .01200 | 49196.0 | .08400 | 95.0 |
| .01250 | 41695.0 | .08600 | 85.0 |
| .01300 | 35654.0 | .08800 | 76.0 |
| .01350 | 30747.0 | .09000 | 68.0 |
| .01400 | 26725.0 | .09200 | 61.0 |
| .01450 | 23400.0 | .09400 | 54.0 |
| .01500 | 20628.0 | .09600 | 49.0 |
| .01550 | 18298.0 | .09800 | 44.0 |
| .01600 | 16324.0 | .10000 | 39.0 |
| .01650 | 14641.0 | .10200 | 36.0 |
| .01700 | 13195.0 | .10400 | 32.0 |
| .01734 | 12315.0 | .10600 | 29.0 |
| .01750 | 12135.0 | .10800 | 26.0 |
| .01800 | 11575.0 | .11000 | 24.0 |
| .02000 | 9605.0 | .11200 | 21.0 |
| .02200 | 7998.0 | .11400 | 19.0 |
| .02400 | 6683.0 | .11600 | 18.0 |
| .02600 | 5602.0 | .11800 | 16.0 |
| .02800 | 4711.0 | .20000 | 0.0 |
| .03000 | 3973.0 | | |
| .03200 | 3361.0 | | |
| .03400 | 2852.0 | | |

TABLE 5 - BREACH FORCE FOR ZONE 6

| T | R(T) | T | B(T) |
|---------|----------|--------|--------|
| 0.00000 | 384.0 | .03500 | 2545.0 |
| .00050 | 706.0 | .03700 | 2135.0 |
| .00100 | 1491.0 | .03900 | 1797.0 |
| .00150 | 2937.0 | .04100 | 1517.0 |
| .00200 | 5800.0 | .04300 | 1285.0 |
| .00250 | 11343.0 | .04500 | 1091.0 |
| .00300 | 21947.0 | .04700 | 929.0 |
| .00350 | 41614.0 | .04900 | 793.0 |
| .00400 | 76017.0 | .05100 | 678.0 |
| .00450 | 130033.0 | .05300 | 582.0 |
| .00500 | 200301.0 | .05500 | 500.0 |
| .00550 | 267029.0 | .05700 | 431.0 |
| .00600 | 302300.0 | .05900 | 373.0 |
| .00616 | 304395.0 | .06100 | 323.0 |
| .00650 | 295349.0 | .06300 | 280.0 |
| .00700 | 259560.0 | .06500 | 243.0 |
| .00750 | 214473.0 | .06700 | 212.0 |
| .00800 | 172277.0 | .06900 | 185.0 |
| .00850 | 137329.0 | .07100 | 162.0 |
| .00900 | 109863.0 | .07300 | 142.0 |
| .00950 | 88691.0 | .07500 | 124.0 |
| .01000 | 72415.0 | .07700 | 109.0 |
| .01050 | 59835.0 | .07900 | 96.0 |
| .01100 | 50018.0 | .08100 | 85.0 |
| .01150 | 42274.0 | .08300 | 75.0 |
| .01400 | 20888.0 | .08500 | 66.0 |
| .01431 | 19380.0 | .08700 | 59.0 |
| .01450 | 18986.0 | .08900 | 52.0 |
| .01500 | 17983.0 | .09100 | 46.0 |
| .01700 | 14514.0 | .09300 | 41.0 |
| .01900 | 11769.0 | .09500 | 37.0 |
| .02100 | 9586.0 | .09700 | 33.0 |
| .02300 | 7841.0 | .09900 | 29.0 |
| .02500 | 6440.0 | .10100 | 26.0 |
| .02700 | 5310.0 | .10300 | 24.0 |
| .02900 | 4395.0 | .20000 | 0.0 |
| .03100 | 3651.0 | | |
| .03300 | 3043.0 | | |

TABLE 6- BREECH FORCE FOR ZONE 7

| T | B(T) | T | B(T) |
|--------|----------|--------|---------|
| .00000 | 2809.6 | .01700 | 13971.0 |
| .00020 | 4589.6 | .01740 | 13354.0 |
| .00060 | 9058.6 | .01780 | 12765.0 |
| .00100 | 18069.0 | .01820 | 12204.0 |
| .00140 | 35565.0 | .01860 | 11668.0 |
| .00180 | 68543.0 | .01900 | 11156.0 |
| .00220 | 126940.0 | .01940 | 10674.0 |
| .00260 | 219070.0 | .01980 | 10214.0 |
| .00300 | 337720.0 | .02020 | 9775.1 |
| .00340 | 446170.0 | .02060 | 9355.5 |
| .00380 | 496900.0 | .02100 | 8954.5 |
| .00420 | 476070.0 | .02140 | 8576.1 |
| .00460 | 411400.0 | .02180 | 8215.1 |
| .00500 | 335660.0 | .02220 | 7869.6 |
| .00540 | 267300.0 | .02260 | 7538.8 |
| .00580 | 211870.0 | .02300 | 7222.5 |
| .00620 | 168900.0 | .02340 | 6924.1 |
| .00660 | 136050.0 | .02380 | 6638.1 |
| .00700 | 110950.0 | .02420 | 6364.5 |
| .00740 | 91613.0 | .02460 | 6102.9 |
| .00780 | 76562.0 | .02500 | 5852.1 |
| .00820 | 64706.0 | .02540 | 5615.3 |
| .00860 | 55253.0 | .02580 | 5389.0 |
| .00900 | 47627.0 | .02620 | 5171.7 |
| .00940 | 41322.0 | .02660 | 4963.0 |
| .00980 | 36281.0 | .02700 | 4763.3 |
| .01020 | 32030.0 | .02740 | 4574.0 |
| .01060 | 29784.0 | .02780 | 4393.7 |
| .01100 | 28358.0 | .02820 | 4220.4 |
| .01140 | 27013.0 | .02860 | 4054.0 |
| .01180 | 25736.0 | .02900 | 3894.2 |
| .01220 | 24521.0 | .02940 | 3743.0 |
| .01260 | 23366.0 | .02980 | 3598.0 |
| .01300 | 22263.0 | .03020 | 3458.6 |
| .01340 | 21237.0 | .04020 | 1361.8 |
| .01380 | 20257.0 | .05020 | 578.4 |
| .01420 | 19324.0 | .06020 | 263.3 |
| .01460 | 18435.0 | .07020 | 128.1 |
| .01500 | 17588.0 | .08020 | 63.5 |
| .01540 | 16794.0 | .09020 | 0.0 |
| .01580 | 16036.0 | .20000 | 0.0 |
| .01620 | 15314.0 | | |
| .01660 | 14626.0 | | |

TABLE 7 - BREACH FORCE FOR ZONE 8

| T | B(T) | T | B(T) |
|---------|----------|--------|---------|
| 0.00000 | 3090.6 | .01700 | 15368.1 |
| .00020 | 5048.6 | .01740 | 14689.4 |
| .00060 | 9964.5 | .01780 | 14041.5 |
| .00100 | 19875.9 | .01820 | 13424.4 |
| .00140 | 39121.5 | .01860 | 12834.8 |
| .00180 | 75397.3 | .01900 | 12271.6 |
| .00220 | 139634.0 | .01940 | 11741.4 |
| .00260 | 240977.0 | .01980 | 11235.4 |
| .00300 | 371491.9 | .02020 | 10752.6 |
| .00340 | 490786.9 | .02060 | 10291.0 |
| .00380 | 546589.9 | .02100 | 9849.9 |
| .00420 | 523676.9 | .02140 | 9433.7 |
| .00460 | 452539.9 | .02180 | 9036.6 |
| .00500 | 369225.9 | .02220 | 8656.6 |
| .00540 | 294029.9 | .02260 | 8292.7 |
| .00580 | 233057.0 | .02300 | 7944.7 |
| .00620 | 185790.0 | .02340 | 7616.5 |
| .00660 | 149655.0 | .02380 | 7301.9 |
| .00700 | 122045.0 | .02420 | 7000.9 |
| .00740 | 100774.3 | .02460 | 6713.2 |
| .00780 | 84218.2 | .02500 | 6437.3 |
| .00820 | 71176.6 | .02540 | 6176.8 |
| .00860 | 60778.3 | .02580 | 5927.9 |
| .00900 | 52389.7 | .02620 | 5688.9 |
| .00940 | 45454.2 | .02660 | 5459.3 |
| .00980 | 39909.1 | .02700 | 5239.6 |
| .01020 | 35233.0 | .02740 | 5031.4 |
| .01060 | 32762.4 | .02780 | 4833.1 |
| .01100 | 31193.8 | .02820 | 4642.4 |
| .01140 | 29714.3 | .02860 | 4459.4 |
| .01180 | 28309.6 | .02900 | 4283.6 |
| .01220 | 26973.1 | .02940 | 4117.3 |
| .01260 | 25702.6 | .02980 | 3957.8 |
| .01300 | 24494.8 | .03020 | 3804.5 |
| .01340 | 23360.7 | .04020 | 1458.0 |
| .01380 | 22282.7 | .05020 | 636.2 |
| .01420 | 21256.4 | .06020 | 289.6 |
| .01460 | 20278.5 | .07020 | 140.9 |
| .01500 | 19346.8 | .08020 | 69.8 |
| .01540 | 18473.4 | .09020 | 0.0 |
| .01580 | 17639.6 | .20000 | 0.0 |
| .01620 | 16845.4 | | |
| .01660 | 16088.6 | | |

DISTRIBUTION

| | <u>Copies</u> |
|---|------------------|
| Defense Documentation Center ATTN: TIPCR Cameron Station Alexandria, VA 22314 | 12 |
| Commander US Army Harry Diamond Laboratories ATTN: AMXDO-EDC AMXDO-SA Washington, DC 20438 | 1 1 |
| Commander US Army Armament Materiel Readiness Command ATTN: DRSAR-LEM Rock Island, IL 61201 | 1 |
| Commander US Army Armament Research & Development Command ATTN: DRDAR-LCW Mr. R. Wrenn DRDAR-LCW Mr. M. Barran DRDAR-SCW-T Mr. E. Larrison Picatinny Arsenal Dover, NJ 07801 | 1 1 1 1 |
| Commander US Army Research Office ATTN: Information Processing Office P.O. Box 12211 Research Triangle Park, NC 27709 | 1 |
| Commander US Army Tank-Automotive Research & Development Command ATTN: Technical Library DRCPM-60 Warren, MI 48090 | 1 1 |
| Commander Project Manager Cannon Artillery Weapons Systems ATTN: DRCPM-CAWS Dover, NJ 07801 | 1 |

Commander
Rock Island Arsenal
ATTN: SARRI-ENW 10
SARRI-EN 1
SARRI-ADL 2
Rock Island, IL 61201

University of Wisconsin-Madison
Department of Mechanical Engineering
ATTN: Dr. S. Wu 5
Madison, WI 53706

